CHEMICAL REVIEWS

Volume 106, Number 1

Large Aqueous Aluminum Hydroxide Molecules

William H. Casey*

Department of Chemistry and Department of Geology, University of California, Davis, California 95616

Received July 8, 2005

Contents

* E-mail: whcasey@ucdavis.edu. Phone: 530-752-3211.

William Casey (born 1955) received his Ph.D. degree in Mineralogy and Geochemistry from The Pennsylvania State University in 1986 under the direction of Prof. Antonio Lasaga. After graduating, he worked as a research geochemist at Sandia National Laboratories in Albuquerque, New Mexico, for several years and jointed the faculty of the University of California in 1991. He has published over 130 scientific articles on subjects relating to aqueous solution chemistry of natural waters, mineral surface chemistry, and reaction kinetics.

1. Introduction

One of the first subjects introduced to students of environmental chemistry is the aqueous chemistry of aluminum. This metal is the third most abundant element in the shallow Earth, where it hydrolyzes in water to produce a rich array of solute molecules and solids, including clays and aluminum hydroxide phases. Although these materials are ubiquitous, we are just beginning to understand the kinetic properties of their surfaces at the molecular scale. The problem is experimental—the solids are too unwieldy, even as colloids, for detailed spectroscopy.

One recent approach has been to use 1−2 nm aqueous Al(III) molecules as experimental models to determine reaction rates and pathways at a fundamental level. The 1−2-nm-sized clusters are useful because they expose functional groups that resemble those found on the minerals, yet reactions at these functional groups can be studied at the molecular scale using relatively simple methods of solution spectroscopy, such as NMR. The 1−2 nm ions are sufficiently small that reactions can then be simulated at a high

10.1021/cr040095d CCC: $59.00
Published on Web 12/07/2005

level using ab initio and molecular-dynamics methods [e.g., ref 1].

In addition to their use as experimental models, these 1−2-nm-sized aluminum hydroxide molecules are familiar to us as the key ingredient in antiperspirants [e.g., ref 2], dye mordants,[3,4] taste astringents, and surfactants [e.g., ref 5]. The polyoxocations are also present in catalysts and clay-pillaring agents [e.g., refs 6−11] and in water-treatment plants. We add them to water to eliminate organic macromolecules and metal pollutants [e.g., refs 12 and 13], and these aluminum hydroxide molecules are not too different from some vaccine adjuvants that we inject into ourselves [e.g., refs 14 and 15].

This paper begins by reviewing the known classes of aluminum hydroxide polyoxocations. It then presents recent kinetic information about their interactions in water.

2. Classes of Large Aqueous Aluminum Hydroxide Clusters

The aluminum hydroxide molecules fall into two broad structural classes. Most familiar are derivatives of the Baker−Figgis−Keggin isomers [Figure 1] that have central metals

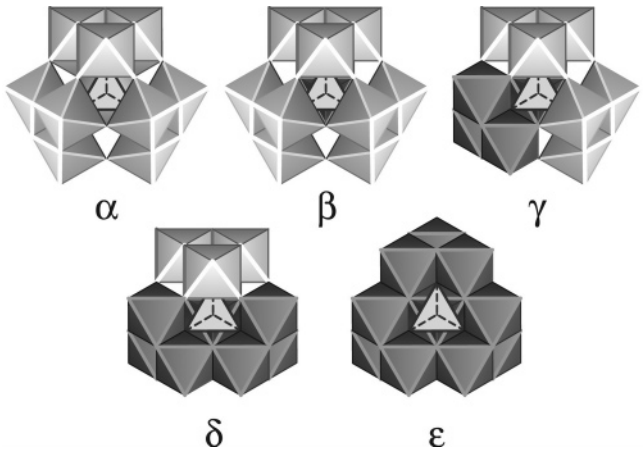

Figure 1. The Baker−Figgis−Keggin isomers shown in polyhedral representation.[16,214] The isomers can be understood as the stepwise rotation of trimeric groups of $Al(O)_6$ octahedra that share corners (light gray) about the μ_4-O so that they share edges with one another (darker gray).

tetrahedrally coordinated to oxygens [$M(O)_4$ sites]. The Baker−Figgis−Keggin isomers are familiar structures among scientists who study polyoxometalates [e.g., refs 16 and 17] and form aluminum molecules having the stoichiometry $MO_4Al_{12}(OH)_{24}(H_2O)_{12}^{7+}$(aq) [M = Ge(IV), Ga(III), or Al(III)].

The second class of oligomers have a characteristic core of edge-shared $Al(O)_6$ octahedra organized into cubane-like moieties that are linked together in a structure similar to the mineral brucite ($Mg(OH)_2$). These molecules are most commonly synthesized with an aminocarboxylate ligand that reduces the overall charge [e.g., refs 18 and 19] but have been found in purely inorganic solutions as well,[20,21] and extensive Fe(III) analogues exist.[22]

It is important to note that these are not the only large aluminum oligomers that are present in a concentrated aluminum solution (see below) but are just the oligomers that can be isolated and for which structural data are available. Most large polymers are yet uncharacterized and unidentified

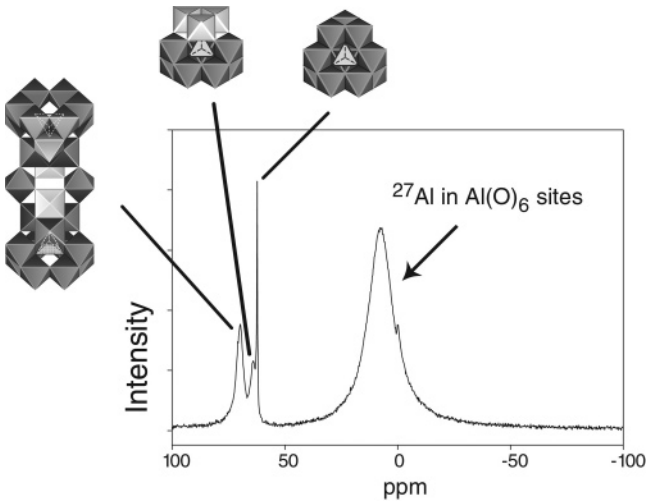

Figure 2. An ^{27}Al NMR spectrum of a hydrolyzed $AlCl_3$ solution showing peaks corresponding to three of the large aluminum molecules, ϵ-**Al$_{13}$**, δ-**Al$_{13}$**, and **Al$_{30}$**. These molecules have a diagnostic peak in the ^{27}Al NMR spectrum because of their relatively symmetric $Al(O)_4$ sites in the center of the molecules. The more abundant $Al(O)_6$ sites yield a broad peak near +10 ppm that is not helpful. These spectra were taken at elevated temperature (~80 °C) to make the peak near +10 ppm particularly conspicuous.

because only complexes with a tetrahedral site yield diagnostic peaks in ^{27}Al or ^{71}Ga NMR spectra [Figure 2].

In the regime of extreme narrowing but slow chemical exchange, the NMR peak widths for ^{17}O and ^{27}Al, the principle NMR nuclei, are dominated by quadrupolar relaxation:

$$\frac{1}{T_2} = \pi(\mathrm{FWHM}) = \frac{3}{40}\frac{2I+3}{I^2(2I-1)}\left[1+\frac{\eta^2}{3}\right][2\pi C_q]^2\tau_c \quad (1)$$

where I is the spin quantum number ($I = {}^5/_2$ for both ^{17}O and ^{27}Al; $I = {}^3/_2$ for ^{69}Ga and ^{71}Ga), C_q is the nuclear quadrupolar coupling constant (the product of the nuclear quadrupolar moment and the maximum component of the electric-field gradient at the nucleus, in hertz), η is the asymmetry of the electric-field gradient (unitless and generally assumed to be zero unless otherwise indicated), and τ_c is the molecular rotational correlation time (s).[23,24] The electric-field gradients at the octahedral aluminum sites [$Al(O)_6$] in most of the oligomers are sufficiently large to yield broad ^{27}Al NMR peaks at $\delta \approx 10$ ppm that are not diagnostic in identification. Only structures with a relatively symmetric ^{27}Al(III), which usually means a tetrahedral $Al(O)_4$ site, yield diagnostic peaks in ^{27}Al NMR spectra.

2.1. Structures with a Central Tetrahedral $M(O)_4$ Site

2.1.1. The ϵ-**Al$_{13}$** Molecule

The ϵ-**Al$_{13}$** ion was originally isolated as sulfate and selenate salts[25−28] and has an ϵ-Keggin-like structure of T_d symmetry, containing a central tetrahedral $Al(O)_4$ unit surrounded by twelve $Al(O)_6$ octahedra. The structure of the ϵ-**Al$_{13}$** can be viewed [Figure 3] as consisting of four planar trimeric $Al_3(OH)_6$ groups that are linked to the central $Al(O)_4$ site via four μ_4-O. The molecule has 12 η-OH_2 sites and two structurally distinct sets of 12 μ_2-OH at the shared edges of $Al(O)_6$ octahedra. These two sets of μ_2-OH differ

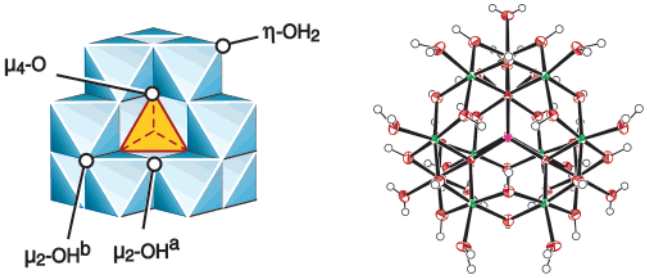

Figure 3. The ϵ-Keggin isomer of the $MO_4Al_{12}(OH)_{24}(H_2O)_{12}^{7+}$-(aq) series of molecules (e.g., ϵ-**Al$_{13}$**) shown in polyhedral representation (left) and as a ball-and-stick model (right). The Al(III) atoms are green, the oxygens are red, and the hydrogens are portrayed as uncolored spheres. The molecule can be viewed as four $Al_3(OH)_6(H_2O)_3$ trimeric groups linked together at polyhedral edges around the central $M(O)_4$ site.

in their positions relative to the μ_4-O groups. One site, labeled μ_2-OH^a, lies cis to two μ_4-O groups [Figure 3]. The other site, labeled μ_2-OH^b, lies cis to one μ_4-O site. One can view these two sites as either linking two trimeric groups together (μ_2-OH^a) or linkages within a single trimeric group (μ_2-OH^b).

The ϵ-**Al$_{13}$** molecule is usually synthesized in a relatively concentrated aluminum solution but can be made over a broad range in concentrations ($1 > \sum[Al] > 10^{-5}$ M) by titrating to $2.1 \leq [OH]/[Al] \leq 2.5$ at 80−90 °C, followed by crystallization with added selenate or sulfate ions. The ϵ-**Al$_{13}$** complex in aqueous solution is easily established from the distinct and narrow peak at 62.5 ppm in ^{27}Al NMR spectra [e.g., refs 29−35]. It can also be detected indirectly by the uptake by phenolic sulfonate ligands and spectrophotometric detection [e.g., ref 36]. The ligand ferron (8-hydroxy-7-iodo-5-quinoline)[32,37−40] and pyrocatechol violet[41] have been used to determine the amount of polymerized aluminum in solution and rely upon the kinetics of reaction [e.g., refs 37 and 42]. Akitt et al.[43] reported a partial molar volume for the ϵ-**Al$_{13}$** molecule, and equilibrium constants are available,[44,45] although it remains questionable as to whether this molecule is truly in reversible exchange equilibrium with other species in solution or it is only a persistent metastable product [see ref 42 and references therein].

2.1.2. Heteroatom ϵ-MAl_{12} Structures

Two decades after Johanssen's work on the ϵ-**Al$_{13}$**, considerable progress was made by the research teams at the University of Freiburg in Germany and Calgary in Canada who independently published a series of papers that examined metal substitutions and polymerization.[46−56] Single-atom substituents include Ge(IV) (yielding $GeO_4Al_{12}(OH)_{24}(H_2O)_{12}^{8+}$ in solution = **GeAl$_{12}$**, refs 46 and 57] and Ga(III) ($GaO_4Al_{12}(OH)_{24}(H_2O)_{12}^{7+}$ = **GaAl$_{12}$**, refs 47−51). Crystals of $Na[GaO_4Al_{12}(OH)_{24}(H_2O)_{12}(SeO_4)_4]\cdot x(H_2O)$, $[GeO_4Al_{12}(OH)_{24}(H_2O)_{12}(SeO_4)_4]\cdot x(H_2O)$, and $Na[AlO_4Al_{12}(OH)_{24}(H_2O)_{12}(SeO_4)_4]\cdot x(H_2O)$ can be grown at 80−90 °C by hydrolysis of the appropriate $AlCl_3$ + MCl_3 solutions followed by filtration, dilution, cooling, and addition of selenate to induce crystallization. The **GeAl$_{12}$** molecule has a slight structural distortion from the cubic symmetry exhibited by ϵ-**Al$_{13}$** and **GaAl$_{12}$** but is overwhelmingly similar.[57]

There is indirect evidence for single-atom substitution of Mn(II)[58] and Fe(III)[59,60] although when Parker et al.[61] attempted to synthesize these and other **MAl$_{12}$** molecules they concluded that only the **GaAl$_{12}$** was unequivocal. This small series has since been augmented with the **GeAl$_{12}$**.[57]

Reports also exist for aluminum-free versions of the ϵ-isomer of the Keggin structure, but none have been crystallized for structural analysis and confirmation. Complexes of Ga(III), $(GaO_4Ga_{12}(OH)_{24}(OH)_{12})^{7+}$,[48,62] have been suggested but not yet isolated [see ref 63]. Similarly, the Fe(III) and Cr(III) analogues[52,53] are suspected but not separated or crystallized.

2.1.3. Transformations of the ϵ-Al_{13} to Other Oligomers

Fu et al.[64] and Nazar et al.[65] showed that other peaks appear downfield in the ^{27}Al NMR spectra as solutions containing the ϵ-**Al$_{13}$** are heated for days at 80−95 °C [see also refs 66 and 67]. Peaks appear near δ = 64.5 ppm, δ = 71.2 ppm, and δ = 75.6 ppm in the ^{27}Al NMR spectra. These authors could enrich solutions in the molecules that yield these peaks by gel-permeation chromatography but could not crystallize the molecules into a material suitable for a structural analysis. The peaks were assigned to AlP_1, AlP_2, and AlP_3 (aluminum peak no. 1, etc.). Fu et al.[64] documented a progressive reaction series where the ϵ-**Al$_{13}$** reacts to form the AlP_1 as an intermediate, then the AlP_2 molecule plus aluminum monomers (the monomers yield a peak near δ = 0 ppm and correspond to $Al(H_2O)_6^{3+}$ and its conjugate base ($Al(H_2O)_5OH^{2+}$) at $4 < pH < 6$). Assignment of the AlP_1 peak is presented in section 2.1.6.

The AlP_2 molecule was more stable than the AlP_1 or ϵ-**Al$_{13}$**, and they interpreted it as a dimer of one of the smaller molecules, probably the ϵ-**Al$_{13}$** cluster.[64] Because the resonance at +64.5 ppm appears and then disappears as peaks at +70.2 and 0 ppm grow, Fu et al.[64] concluded that the AlP_1 complex is a transient intermediate. Parker et al.[61] showed that the **GaAl$_{12}$** molecule could not be converted into an AlP_2 equivalent, indicating that the central Ga(III) atom considerably stabilized the structure. Both Fu et al.[64] and Parker et al.[61] report apparent pseudo-first-order rate coefficients for the polymerization of ϵ-**Al$_{13}$** into the AlP_2 oligomer at 80 °C of about $(0.036-0.05) \times 10^{-2}$ h^{-1} (see also refs 68 and 69).

2.1.4. The δ-Al_{13} Molecule

Of the five Baker−Figgis−Keggin isomeric structures [Figure 1], the δ-Keggin isomer of the Al_{13} molecule (δ-**Al$_{13}$**) is the only other aluminum oligomer besides the ϵ-**Al$_{13}$** that has yet been synthesized in isolation and structurally characterized (see below). The δ-**Al$_{13}$** molecule has a single $[Al_3O_{13}]$ trimeric group rotated 60° around the μ_4-O [Figure 4] so that it bonds at polyhedral corners, not at

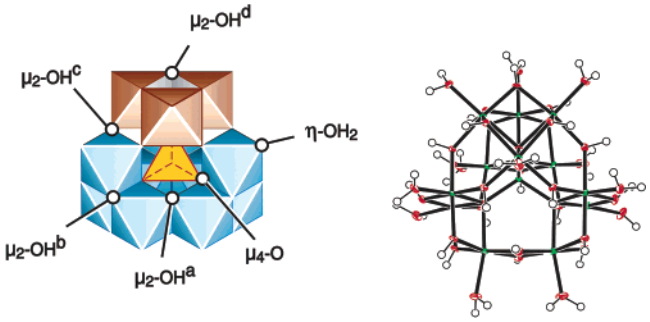

Figure 4. The δ-**Al$_{13}$** molecule shown in polyhedral representation (left) and as a ball-and-stick model (right).[70] The molecule is similar to the ϵ-**Al$_{13}$** but with one trimeric group (shown in brown) rotated 60° so that it bonds via octahedral corners, not edges. Some of the structurally distinct hydroxyl bridges are identified. The Al(III) atoms are green, the oxygens are red, and the hydrogens are portrayed as uncolored spheres.

the edges. All three other [Al_3O_{13}] trimers in the molecule join at shared edges, as in the ϵ-**Al$_{13}$**. Rowsell and Nazar[70] isolated this δ-**Al$_{13}$** isomer structure, along with the large **Al$_{30}$** molecule discussed in the next section.

The δ-**Al$_{13}$** structure has more types of oxygens than the ϵ-**Al$_{13}$** molecule because of the introduction of the corner-shared μ_2-OH and the resulting reduction in symmetry from T_d to C_{3v}. For example, the δ-**Al$_{13}$** contains three distinct sets of η-OH_2 and two types of μ_4-O, based upon their positions relative to the rotated trimer. Rowsell and Nazar[70] conclude that the δ-**Al$_{13}$** molecule accounts for the AlP_1 peak of Fu et al.[64] and yields a peak in the ^{27}Al NMR spectrum near δ = 64.5 ppm [see also refs 68, 69, and 71].

2.1.5. α-*Al$_{13}$* Structures

The only aluminum oligomer that forms in one of the Baker−Figgis−Keggin isomers is in the mineral zunyite [Figure 5], which has the stoichiometry $Al_{13}Si_5O_{20}(OH)_{16}F_2Cl$ and is a modified form of the α-**Al$_{13}$**. This mineral is found near hydrothermal ore deposits, can be synthesized hydrothermally [e.g., ref 72], and was first studied by Pauling.[73] The mineral is used extensively for structural [e.g., ref 74] and spectroscopic studies [e.g., refs 75−78], but the α-**Al$_{13}$** has not yet been isolated as a solute or as a molecule in a simple salt. The silicate groups are directly bonded to the α-**Al$_{13}$** in zunyite.

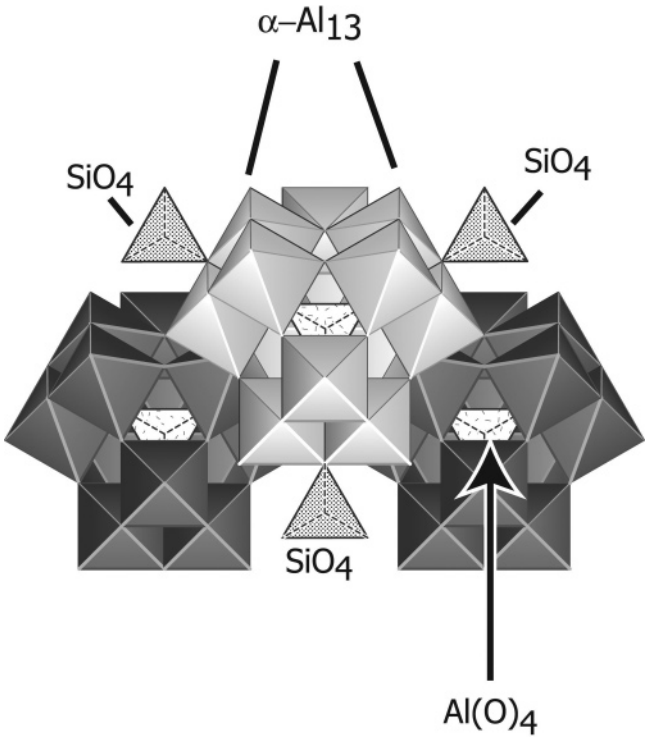

Figure 5. The mineral zunyite, with the nominal stoichiometry $Al_{13}Si_5O_{20}(OH)_{16}F_2Cl$, is the only occurrence of the α-**Al$_{13}$** isomer of the Baker−Figgis−Keggin series. The mineral contains α-**Al$_{13}$** clusters (shown here in both light and dark gray) with silicate chains bonded sharing some hydroxyl bridges in μ_3-OH coordination. The silicate groups are shown as hatched-pattern tetrahedra.

2.1.6. The $Al_2O_8Al_{28}(OH)_{56}(H_2O)_{26}^{18+}$(aq) (*Al$_{30}$*) Molecule

An exceptional advance in identifying aqueous aluminum polymers was the isolation and structural characterization by two independent groups[70,71] of the largest aluminum polyoxocation yet characterized, the **Al$_{30}$** molecule [**Al$_{30}$** = $Al_2O_8Al_{28}(OH)_{56}(H_2O)_{26}^{18+}$(aq)], which also accounts for the AlP_2 peak of Fu et al.[64] and Nazar et al.[65] The **Al$_{30}$** is ∼2 nm in length [Figure 6] and exposes oxygens in many different coordination environments to the aqueous solution. The ^{27}Al NMR spectrum shown by Akitt and Mann[66] showed the presence of this **Al$_{30}$** molecule as a broad peak near 71 ppm, which is also evident in Akitt and Farthing[29] and Akitt et al.[67] Similarly, Allouche and Taullele[79] show conspicuous peaks at 76 and 81 ppm in the ^{27}Al NMR spectra of their **Al$_{30}$** solutions. Shafran and Perry[68] also report minor peaks at 74, 48, and 81 ppm. As all the authors state, these peaks correspond to polymers with a higher molecular weight than the **Al$_{30}$** that have yet to be isolated and crystallized.

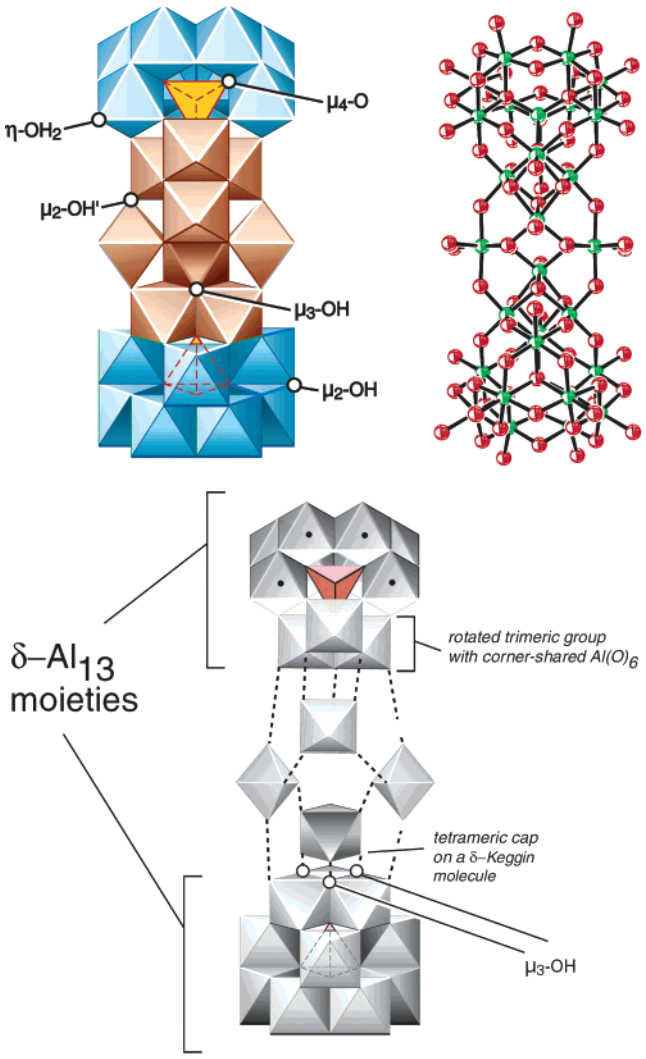

Figure 6. The $Al_2O_8Al_{28}(OH)_{56}(H_2O)_{26}^{18+}$(aq) (**Al$_{30}$**) molecule shown in polyhedral representation (top left), as a ball-and-stick model (top right) and in a polyhedral exploded view (bottom). Hydrogens are eliminated from the structure for the sake of clarity.[70,71] The **Al$_{30}$** molecule can be viewed as two δ-**Al$_{13}$** molecules joined via a belt of four joining $Al(O)_6$ octahedra. The blue polyhedra are organized in a similar fashion as the ϵ-**Al$_{13}$**. In the ball-and-stick diagram, the Al(III) atoms are green and the oxygens are red.

Fu et al.[64] suspected that the AlP_3 peak corresponded to a dimer made of two ϵ-**Al$_{13}$** that were bonded and rotated to yield a compound with molecular weight near 1500−3000 Da, having the approximate stoichiometry $Al_{24}O_{72}$. These conclusions were insightful—the structure of the **Al$_{30}$** is best

understood as two δ-**Al$_{13}$** molecules that face one another at the rotated trimers and are bonded via a belt of additional $Al(O)_6$ linkages [Figure 6]. One set of linkages consists of $Al(O)_6$ groups that share three edges at the apices of the two δ-**Al$_{13}$** units, forming a nonplanar tetrameric cap on each of the two δ-**Al$_{13}$**-like molecules. These linkages form three adjacent μ_3-OH groups on each tetrameric subunit. The second linkage set consists of $Al(O)_6$ groups that connect the two modified δ-**Al$_{13}$** molecules to one another at the tetramer caps via four corner-shared μ_2-OH bridges.

The disruption of symmetry creates many sets of different oxygens. In fact, Allouche et al.[71] found evidence that the **Al$_{30}$** sulfate salt exhibits C_c space-group symmetry, which requires all 88 oxygens to be inequivalent. If instead we can assume that the molecule has C_{2h} symmetry, we can identify 15 sets of inequivalent hydroxyl bridges in the **Al$_{30}$** and eight distinct sets of bound waters [see ref 80]. The eight total μ_4-O sites in the **Al$_{30}$** link the two tetrahedrally coordinated aluminums [$Al(O)_4$] to the outer part of the molecule.

Allouche and Taullele[79] and Shafran and Perry[68,69] conducted time-series studies and showed that the **Al$_{30}$** complex can be easily formed by heating a solution of ϵ-**Al$_{13}$** at 85 °C for a few days. However, it also forms during storage of a stock millimolar solution of ϵ-**Al$_{13}$** for a decade or so (see Figure 9 in ref 81), and this **Al$_{30}$** molecule can be a component of some commercial aluminum chlorhydrate [$Al_2(OH)_5Cl$], along with the ϵ-**Al$_{13}$** [e.g., ref 81]. As mentioned above, there is apparently no Ga(III)-centered analogue of the **Al$_{30}$**, although the **GaAl$_{12}$** is apparently more stable than the **Al$_{30}$**. It worth revisiting this question of a **GaAl$_{28}$** molecule with new experiments since Parker et al.[61] report a decrease in intensity of the peak associated with the $Ga(O)_4$ in the ^{71}Ga NMR spectra with aging at 80−90 °C, suggesting that polymerization into a larger molecule was occurring. A more detailed study might uncover this polymerization and isolate the resulting molecule using one of the new supramolecular[63] or column[82] methods that are being developed.

Allouche et al.[83] employed a triple-quantum ^{27}Al-MAS NMR method to assign eight peaks in the ^{27}Al NMR spectrum. Narrow peaks at $\delta = 68.8$ ppm and $\delta = 69.9$ ppm were assigned to the two $Al(O)_4$ and indicate that the structure is not centrosymmetric. The remaining $Al(O)_6$ peaks exist as six groups with peak positions ranging from $\delta \approx 4$ to $\delta \approx 12$ ppm and with quadrupolar-coupling constants ranging from ~500 to ~1600 kHz.[83]

2.1.7. Heteroatom Derivatives of the *Al$_{30}$*

Recent efforts created nanocluster composites using the ϵ-**Al$_{13}$**,[84−86] the δ-**Al$_{13}$** and **Al$_{30}$** molecules,[87] and the ϵ-**GaAl$_{12}$** molecules,[88] along with tungstate or molybdate polyoxoanions. The clusters bond to one another in the composite by electrostatic interaction and via hydrogen bonding, and they create a porous solid with interesting properties. Son et al.[87] showed that the **Al$_{30}$** molecule exchanges metals in a composite with the $H_2W_{12}O_{40}^{6-}$ (**W$_{12}$**) polyoxoanion to form a new compound, **W$_2$Al$_{28}$**, that is nearly isostructural with the **Al$_{30}$** structure [Figure 7]. This new compound differs in that a $W(O)_6$ group replaces one of the capping $Al(O)_6$ groups at each end of the **Al$_{30}$** molecule.

The fact that this **W$_2$Al$_{28}$** molecule broadly resembles the dimer-like structure of the wider family of tungstate clusters [e.g., refs 16, 89, and 90] suggests that more varieties of tungstoaluminate clusters could be synthesized [Figure 7].

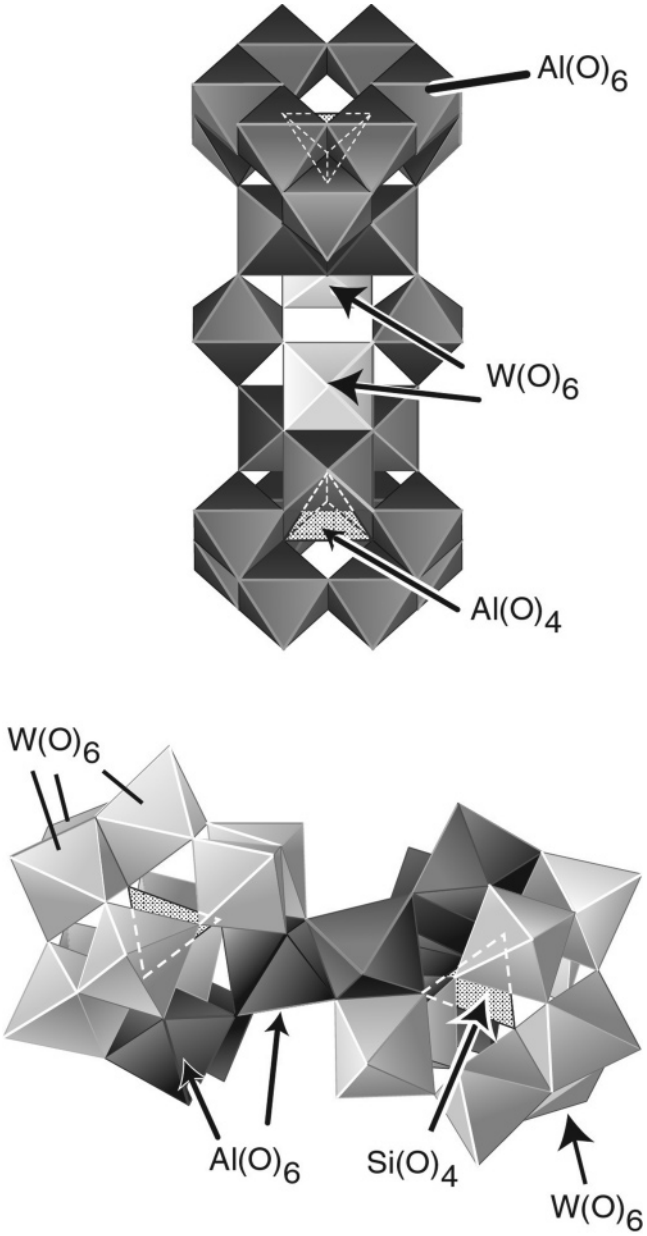

Figure 7. The Al(III) → W(VI) substitution (and the reverse) into the largest tungstate and aluminate clusters might be a fruitful area for research. The structure of the $W_2Al_{28}O_{18}(OH)_{48}(H_2O)_{24}^{12+}$ ion (**W$_2$Al$_{28}$**) shown in polyhedral representation (top) is nearly isostructural with the **Al$_{30}$** ion. The $Al(O)_6$ groups are shown in dark gray, and the $W(O)_6$ groups are shown as light gray. The $Al(O)_4$ site in the center of the molecules is hatched. In the bottom figure, the $H_{14}Si_2W_{18}Al_6O_{37}(H_2O)_{12}$ cluster can be considered as an altered dimer of two aluminum-substituted and $Si(O)_4$-centered tungstate clusters in the α-Keggin structure.[215] One trimeric group of the four in each α-W_{13} Keggin structure is replaced by a group of three $Al(O)_6$. The two dimers then link across a shared edge of two $Al(O)_6$ groups.

Similarly, there are several classes of heteropolyanions that contain aluminum substituents, either as the tetrahedral core of a molecule with one of the Keggin isomer structures [e.g., ref 91] or as an $Al(O)_6$ heteroatom substituent in the outer part of a tungsten or molybdate Keggin isomer structure [e.g., refs 92−95]. Son et al.[87] demonstrated that aluminum-rich tungstate clusters could be synthesized based upon the aluminum polyoxocations of the Keggin class, such as the **Al$_{30}$**.

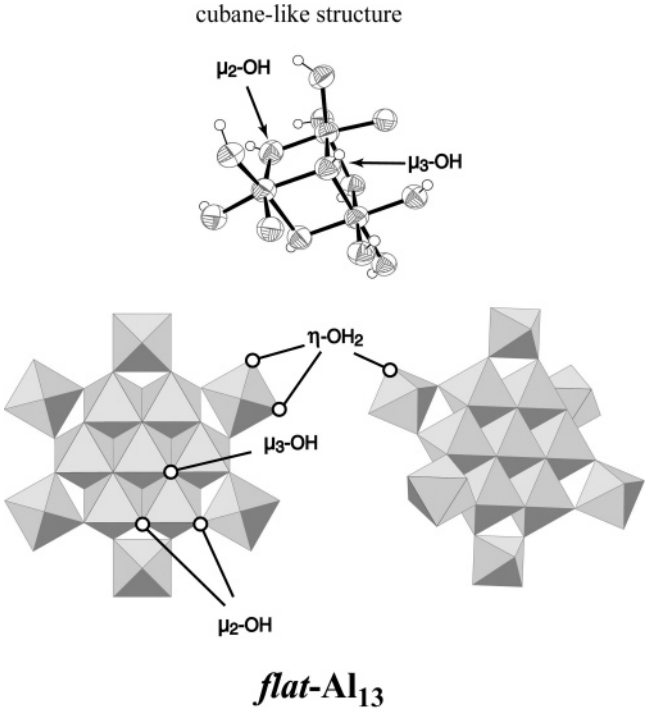

Figure 8. A new series of aqueous aluminum clusters is based upon a repeated set of cubane-like moieties (top) arrayed in a lattice of edge-shared $Al(OH)_6$ octahedra similar to the brucite lattice.[96] Three such molecules have been synthesized, having either 8, 13, or 15 aluminums, but several other molecules have been made from other trivalent metals (i.e., Fe(III) and Ga(III), see ref 96). The **flat-Al$_{13}$** has the core structure $Al_{13}(\mu_3\text{-}OH)_6(\mu_2\text{-}OH)_{18}(H_2O)_6^{15+}$ and is shown at bottom in polyhedral representation. The **flat-Al$_{13}$** has been synthesized using chloride salts to give the $Al_{13}(\mu_3\text{-}OH)_6(\mu_2\text{-}OH)_{18}(H_2O)_6^{15+}$ ion[20,21] and employing heidi as a tetradentate chelating ligand,[18] which bonds at the six corner-shared $Al(O)_6$ groups, giving $Al_{13}(\mu_3\text{-}OH)_6(\mu_2\text{-}OH)_{12}(H_2O)_6(heidi)_6^{3+}$ ion.

2.2. Molecular Clusters Based upon Brucite-like $Al_3(OH)_4^{5+}$ Cores

Other aluminum clusters have been isolated in the past decade that are based upon a periodic array of alternating Al(III) and hydroxyl linkages in cubane-like moieties [Figure 8] arrayed in edge-shared $Al(O)_6$ similar to brucite [see ref 96]. These molecules have no central $Al(O)_4$ site and thus are difficult to detect in an ^{27}Al NMR spectrum because the $Al(O)_6$ sites yield broad peaks. The purely inorganic salts are also difficult to crystallize, and the only ion stoichiometries that have yet been reported are the octamer **Al$_8$**, $Al_8(\mu_3\text{-}OH)_2(\mu_2\text{-}OH)_{12}(H_2O)_{12}^{10+}$ [97] and the **flat-Al$_{13}$**, $Al_{13}(\mu_3\text{-}OH)_6(\mu_2\text{-}OH)_{18}(H_2O)_6^{15+}$.[20,21] The latter ion probably forms one of the salts in the early study by Breuil [ref 98; F. Taulelle, personal communication] and can be synthesized in large quantities by hydrothermal reaction. In their core structure, these clusters resemble somewhat the Anderson-type structures, which are familiar in molybdate chemistry (e.g., $Al(OH)_6Mo_6O_{18}^{3-}$; see refs 92 and 93) and consist of linked $M(O)_6$ octahedra surrounding a central $Al(O)_6$. In the aluminomolybdates, however, there are no corner-shared $Al(O)_6$, as in these brucite-like molecules.

Although the purely inorganic salts are difficult, the synthesis is much easier if the molecules are ligated at the edges by organic anions that reduce the molecule charge. Much work on this subject has been done by the research groups of Profs. Powell and Heath at Universities of Karlsruhe and Manchester, respectively, who showed that similar Al(III), Ga(III), and Fe(III) clusters can be stabilized using aminocarboxylate ligands [e.g., refs 18, 19, 22, and 99−101]. For aluminum clusters, two ion stoichiometries have been synthesized, $Al_{13}(\mu_3\text{-}OH)_6(\mu_2\text{-}OH)_{12}(H_2O)_6(heidi)_6^{3+}$ (heidi = *N*-(2-hydroxyethyl)iminodiacetic acid, see refs

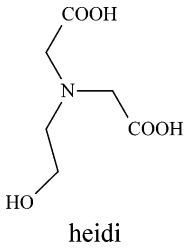

heidi

18, 19, 22, 99, and 101) and **Al$_{15}$**, $Al_{15}(\mu_3\text{-}O)_4(\mu_3\text{-}OH)_6(\mu_2\text{-}OH)_{14}(hdpta)^{3-}$ (H_5hpdta = 2-hydroxypropane-1,3-diamine-*N*,*N*,*N*′,*N*″-tetraacetic acid.[101] To distinguish these molecules from the ϵ-**Al$_{13}$** molecule, I refer to the inorganic chloride salt as the **flat-Al$_{13}$** and the heidi-ligated structure as the **flat-Al$_{13}$−heidi**.

Goodwin et al.[96] argued that a wide range of metal hydroxide clusters are built upon this hypothetical brucite-like lattice, including clusters of Fe(III), Al(III), Mn(III), and Ga(III) with 7, 8, 13, 15, 17, 19, and 21 metals. The relation between this hypothetical $Al(OH)_3$ brucite lattice and the cluster structure is illustrated in Figure 9, where we relate

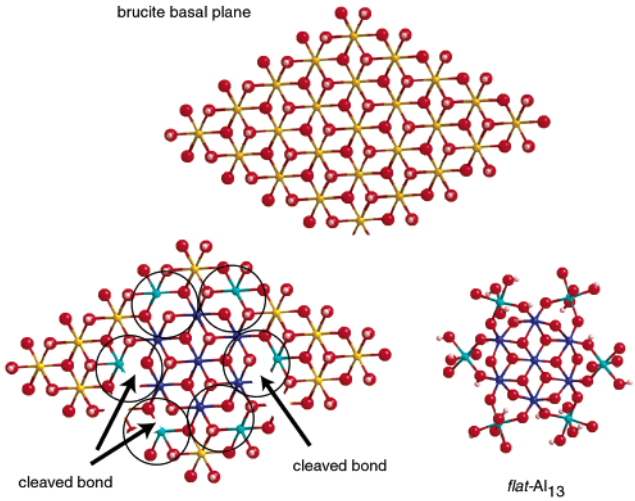

Figure 9. Aluminum and many other metal hydroxide clusters[96] can be built as fragments of a hypothetical brucite-like lattice made of trivalent metals linked by μ_3-OH. An $Al(OH)_3$ solid built on the brucite ($Mg(OH)_2$) lattice is shown at the top with the Al(III) as gold, the oxygens red, and the hydrogens as white spheres. To generate the **flat-Al$_{13}$** clusters (bottom right), a hexagonal array of $Al(OH)_6$ groups (light-blue atoms) has one bond to a μ_3-OH replaced with a water molecule and three bound waters truncating them. The Al(III) atoms in the core (dark-blue) retain their brucite-like structure, while the light-blue atoms bond to the next row of $Al(O)_6$ via μ_2-OH. In the clusters synthesized with aminocarboxylates (e.g., the **flat-Al$_{13}$−heidi** and **Al$_{15}$**).

the **flat-Al$_{13}$** structure of Seichter et al.[20] to a brucite basal plane. The metal atoms are arranged on a hexagonal array with six of the outermost $Al(OH)_6$ groups having a single bond to the μ_3-OH cleaved and replaced with a bound water molecule to retain the octahedral coordination. The result is a molecule with a central cubane-like core with corner-shared $Al(O)_6$ at the edges. Although the **Al$_8$** is the smallest cluster of this series, the Al(III)−citrate trimer isolated and crystal-

lized by Feng et al.[102] bears some similarity to the structure in that one $Al(O)_6$ site is corner-shared to the other two $Al(O)_6$, which share edges via two μ_2-OH [see also refs 81 and 99].

Ligation to the aminocarboxylates does not change the core structure of linked $Al(O)_6$ in a brucite-like arrangement. The aminocarboxylate ligands are tetradentate and replace the outer four water molecules in each of the peripheral corner-shared $Al(O)_6$ groups. Thus, the **flat-Al$_{13}$** molecule in chloride salt has the same core structure as the **flat-Al$_{13}$−heidi**, but the tetradentate heidi replaces bound waters. In the **flat-Al$_{13}$**, bound water molecules exist that are both cis and trans to a μ_2-OH and are hence expected to be kinetically distinct. In the **Al$_8$** molecule, a second set of water molecules is bound to edge-shared $Al(O)_6$ in the core. These water molecules are trans to a μ_3-OH and cis to four μ_2-OH and are hence expected to be anomalously labile. In the **Al$_{15}$** structure, there are no bound waters, and this material is relatively insoluble.

The **Al$_8$**, **flat-Al$_{13}$**, and **Al$_{15}$** molecules are ill-suited for standard solution ^{27}Al NMR studies because there is no highly symmetric site in the cubane-like structures, such as the $Al(O)_4$ in the **ϵ-Al$_{13}$** molecule, that yields a distinctive peak in the ^{27}Al NMR spectrum. Furthermore, both the **flat-Al$_{13}$** and **Al$_8$** molecules decompose in most aqueous solutions, rendering ^{17}O NMR studies of their reactivity impossible. However, multiquantum ^{27}Al-MAS NMR (MQMAS) has proven useful, and a key study was that of Allouche et al.,[83] who related peak positions and quadrupolar-coupling constants to structural aluminum positions in salts of the **ϵ-Al$_{13}$**, the **Al$_{30}$**, and the **flat-Al$_{13}$** clusters. For the **flat-Al$_{13}$**, there are six different aluminum sites in the core structure. The central $Al(\mu_3\text{-}OH)_6$ site has a relatively sharp ^{27}Al NMR resonance in MQMAS at $\delta = 11.7$ ppm. The surrounding ring of $Al(\mu_3\text{-}OH)_2(\mu_2\text{-}OH)_3(H_2O)$ yields peaks at $\delta = 13.3$ ppm and $\delta = 13.9$ ppm. Finally, the six peripheral $Al(O)_6$ that share corners with adjacent $Al(O)_6$ in polyhedral representation have peaks of $\delta = 2.9$ and 3.1 ppm. Casey et al.[97] made a generally similar set of assignments for the **Al$_8$** at 11.7 T. They report that the core aluminums have chemical shifts near $\delta = 13 \pm 1$ ppm and C_q values near 6 MHz, which are close to the values for similar sites in the **flat-Al$_{13}$** molecule.[83,93] Likewise, the remaining outer $Al(O)_6$ sites closely resemble those in the periphery of the **flat-Al$_{13}$** that are linked to two μ_2-OH and four η-H_2O. They assigned these peripheral $Al(O)_6$, sharing corners with adjacent $Al(O)_6$, to $\delta = 6-7$ ppm.

2.3. Alumoxanes

Alumoxanes form from the hydrolysis of organoaluminum compounds to yield cagelike aluminum structures with μ-oxo and μ-hydroxo bridges and terminal organic ligands [see refs 103 and 104]. Most alumoxanes decompose rapidly in water and are thus beyond the scope of this article. A few hydrolytically stable carboxylate-bridged alumoxanes have been synthesized. Barron's group[105−108] isolated alumoxanes by reaction of carboxylic acids with boehmite [γ-AlOOH, see also ref 109]. However, Callender et al.[109] point out that the water-soluble alumoxanes are better thought of as carboxylate-stabilized colloids and not as aqueous clusters of uniform stoichiometry and structure. These molecules could be profoundly useful as kinetic models for aqueous reactions if metastable monospecific solutions could be prepared.

2.4. New Methods of Aluminum and Heteroatom Cluster Isolation

The supramolecular methods of synthesis hold great promise for isolating the large aluminum hydroxide clusters, and progress toward this goal was achieved by Drljaca et al.[110] and Hardie and Raston[111] who showed that the **ϵ-Al$_{13}$** molecule could be trapped in a calixarene/8-crown-6-ether combination. A new method of isolating Ga(III) clusters was reported by Gerasko et al.,[63] who crystallized the **flat-Ga$_{13}$** molecule (structurally analogous to the **flat-Al$_{13}$**) and discovered a new large **Ga$_{32}$** ion $[Ga_{32}(\mu_4\text{-}O)_{12}(\mu_3\text{-}O)_8(\mu_2\text{-}OH)_{39}(H_2O)_{20}^{17+}]$ that has a unique structure. The **Ga$_{32}$** contains two pairs of corner-shared $Ga(O)_4$ sites surrounded by $Ga(O)_6$ arranged in trimeric clusters like the **ϵ-Al$_{13}$** and **ϵ-Ga$_{13}$** molecules. This **Ga$_{32}$** structurally resembles a gallium version of the AlP_2 molecule originally imagined by Fu et al.[64] that has since been identified as the **Al$_{30}$**.

These new supramolecular clusters could potentially isolate many more aluminum molecules from a hydrolyzed solution. The Gerasko et al. group has also been able to isolate the **Al$_{30}$** and **flat-Al$_{13}$** molecule using their cucurbit supramolecule (V. Fedin, personal communication) but have not yet identified any new aluminum clusters. Rather et al.[112] established a method of crystallizing the **flat-Ga$_{13}$** molecule $[Ga_{13}(\mu_3\text{-}OH)_6(\mu_2\text{-}OH)_{18}(H_2O)_6^{15+}]$ by slow hydrolysis of an organonitrate and have since also synthesized the **flat-Al$_{13}$** using this method (D.W. Johnson, personal communication).

3. Kinetics of Ligand-Exchange Reactions in Aluminum and Heteroatom Clusters

3.1. The Analogy to Aluminum Hydroxide Mineral Surfaces

The similarity of at least some features of these molecules and aluminum hydroxide soil minerals can be restated. Consider the Brønsted acidities, which influence many of the surface properties of the minerals. When fully protonated, minerals such as gibbsite or bayerite [γ-$Al(OH)_3$] have surface proton charge densities of 0.16−0.48 C/m^2.[113,114] The surface charge density of fully protonated **ϵ-Al$_{13}$** is 0.32 C/m^2, and the **flat-Al$_{13}$** molecule has a charge density of ∼1.2 C/m^2, which is, of course, reduced by ligation to the heidi ligand.

It is also important that the cubane-like aluminum hydroxide clusters (**Al$_8$**, **flat-Al$_{13}$**) are broadly similar to minerals of the hydrotalcite class, which are catalysts and are environmentally important. The hydrotalcites are layered structures composed of positively charged, brucite-type metal hydroxide layers intercalated with anions and water molecules. These minerals are important to environmental chemistry because they form quickly in some metal-contaminated environments as aluminum released by dissolving soil minerals combines with the pollutant metal.

3.2. Oxygen-Isotope Exchange Rates

In this section, I review some recent kinetic data using the aluminum hydroxide clusters described above. All work to date has employed the small ϵ-isomers in the **MAl$_{12}$** series (**ϵ-Al$_{13}$**, **GaAl$_{12}$**, and **GeAl$_{12}$**) and the **Al$_{30}$** molecule, which is less useful because of its structural complexity. In ^{17}O NMR studies, sulfate or selenate salts of the **ϵ-Al$_{13}$**, **GaAl$_{12}$**, and **GeAl$_{12}$** are dissolved metathetically in the presence of $BaCl_2$ to release the polyoxocation ions into an ^{17}O-enriched

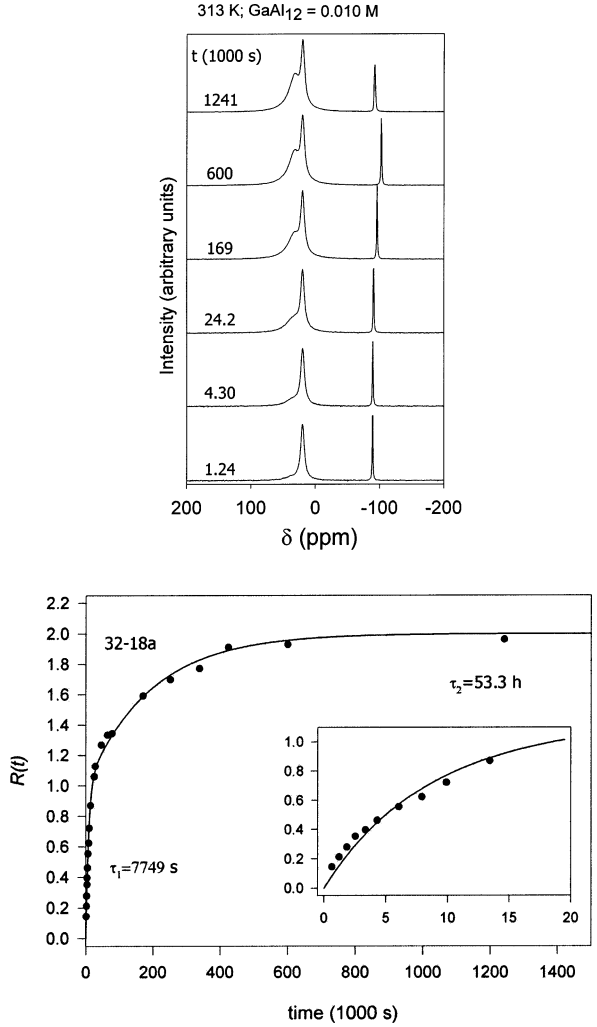

Figure 10. (top) ^{17}O NMR spectra at 313 K as a function of time for a ~0.010 M solution of **GaAl$_{13}$** with 0.25 M Mn(II) added to remove the bulk water peak.[119] Vertical scaling is normalized to the integrated intensity of the peak near −100 ppm, which corresponds to an external, coaxial $TbCl_3$(aq) insert that was used as an intensity standard. The peak near +22 ppm corresponds to bound water molecules in the **GaAl$_{12}$** complex. The broader downfield peak that increases in intensity with time arises from the two μ_2-OH sites in the molecule, which react at different rates. Missing is the peak that would correspond to the four μ_4-O, indicating that these sites are inert to exchange. (bottom) The reduced intensity ($R(t) = I_{\delta=35ppm}/I_{\delta=22ppm}$) grows in a biexponential manner and ultimately reaches $R(t) = 2$, corresponding to the intensity of two sets of 12 fully exchanged μ_2-OH ($\delta = 35$ ppm) divided by the intensity in one set of 12 fully exchanged η-OH_2 ($\delta = 22$ ppm). The ratio corresponds to the stoichiometry GaO_4Al_{12}-$(\mu_2\text{-}OH)_{24}(\eta\text{-}OH_2)_{12}^{7+}$. The biexponential growth indicates that μ_2-OH^a and μ_2-OH^b react at different rates, and the inset shows the earliest times, as $R(t) \rightarrow 1$, corresponding to exchange of the first set of μ_2-OH. Casey and Phillips[119] used eq 1 and a value of $\tau_c = 130$ ps from ref 116 to calculate C_q values of 8.7 and 6.5 MHz for the two μ_2-OH sites in the dissolved **GaAl$_{12}$** molecule.

solution. Changes in ^{17}O NMR peak intensities [Figure 10] then provide information about rates of exchange of μ_2-OH^a and μ_2-OH^b sites, and rate parameters for exchange of bound waters can be determined using the ^{17}O-line-broadening method.[115] The μ_4-O sites in the center of the ϵ-**Al$_{13}$**, **GaAl$_{12}$**, and **GeAl$_{12}$** would appear at +55 ppm[116] in a ^{17}O NMR spectrum and yet are missing when the **MAl$_{12}$** salts are dissolved in ^{17}O-enriched water, indicating that these μ_4-O are inert to isotopic exchange. This peak at +55 ppm only appears in the ^{17}O NMR spectra when the ϵ-**Al$_{13}$**, **GaAl$_{12}$**, and **GeAl$_{12}$** oligomers are completely dissociated into monomers in ^{17}O-enriched water by acidification and then reassembled back into the polyoxocation by base addition.

Because the μ_4-O sites are inert to exchange, the rates of steady exchange of all other oxygens in the molecules can be measured and these exchanges can be distinguished from dissolution and reformation of the molecule. In fact, virtually all other oxygen sites exchange several times with bulk solution before the molecule dissolves. The ^{17}O NMR spectra exhibit a peak near +20 ppm that is assignable to the 12 bound water molecules. This peak appears instantaneously in the spectra and has a constant intensity. A second peak near +35 ppm grows with time [Figure 10], and the peak exhibits a distinctly biexponential rate of growth. This +35 ppm peak is assigned to two resonances that cannot be resolved from one another and that correspond to the two sets of 12 μ_2-OH in the ϵ-**Al$_{13}$**, **GaAl$_{12}$**, and **GeAl$_{12}$** oligomers.[117−120] Although the two resonances that contribute to the +35 ppm peak cannot be resolved from one another, they are kinetically distinct and are identified as μ_2-OH^{fast} and μ_2-OH^{slow} so as not to confuse them with the structural positions, μ_2-OH^a and μ_2-OH^b. Although the μ_2-OH^{fast} and μ_2-OH^{slow} sites cannot yet be unequivocally assigned to the μ_2-OH^a and μ_2-OH^b sites within each of the molecules, it is reasonable to assume that the μ_2-OH^{slow} site corresponds to the μ_2-OH^b sites and the μ_2-OH^{fast} sites correspond μ_2-OH^a.

There are considerable differences in the reactivities of the hydroxyl bridges both within a single molecule and between the same site in the set of isostructural molecules (ϵ-**Al$_{13}$**, **GaAl$_{12}$**, and **GeAl$_{12}$**). Characteristic times for exchange of the μ_2-OH^{fast} and μ_2-OH^{slow} sites in the **GaAl$_{12}$** molecule at 298 K are $\tau_{298} \approx 15.5$ h and $\tau_{298} \approx 680$ h, respectively,[119] whereas the corresponding times are $\tau_{298} \approx 1$ min and $\tau_{298} \approx 17$ h for the ϵ-**Al$_{13}$** molecule.[117,118] The μ_2-OH^{fast} bridge in the **GeAl$_{12}$** molecule exchanges at rates too fast to measure,[120] but the other has $\tau_{298} \approx 25$ min. For within the ϵ-**Al$_{13}$** complex, $\tau_{298}^{fast}/\tau_{298}^{slow} \approx 10^3$, but for the **GaAl$_{12}$** molecule, $\tau_{298}^{fast}/\tau_{298}^{slow} \approx 44$. Thus, the difference in reactivities of these two structural sites is profound. Extrapolated to 298 K, the observed rates of exchange of μ_2-OH sites in these molecules spans a factor of $\sim 10^5$ and is probably much larger if the more reactive set of μ_2-OH sites in the **GeAl$_{12}$** molecule could be included. The lifetimes of the bound water molecules, however, fall close to one another ($\tau_{ex}^{298} \approx 10^{-3}$ s) in the series ϵ-**Al$_{13}$**, **GaAl$_{12}$**, and **GeAl$_{12}$** and are near values measured for simple aluminum monomer complexes [Table 2].

With the exception of the datum for the μ_2-OH^{fast} in the ϵ-**Al$_{13}$** molecule [Table 1], the activation enthalpies fall into a range similar to those corresponding to the dissociation of a hydroxyl bridge in simple inert-metal dimers; that is, $\Delta H^{\ddagger} \approx 100$ kJ mol^{-1}, and $\Delta S^{\ddagger}$ is near zero.[121] The values of $\Delta H^{\ddagger}$ and $\Delta S^{\ddagger}$ for the μ_2-OH^{fast} in the ϵ-**Al$_{13}$** molecule are extraordinarily high ($\Delta H^{\ddagger} \approx 204$ kJ mol^{-1}; $\Delta S^{\ddagger} \approx 400$ J mol^{-1} K^{-1}) and may account for the large differences in $\tau_{298}^{fast}/\tau_{298}^{slow}$ for this molecule relative to the **GaAl$_{12}$**.

High-pressure data are available for the **GaAl$_{12}$**, and the ^{17}O NMR line widths of bound waters decrease from 0.1 to 350 MPa, yielding an activation volume of $\Delta V^{\ddagger} = +3 \pm 1$ cm^3 mol^{-1},[122] which is smaller than the value for the $Al(H_2O)_6^{3+}$ complex (+5.7 cm^3 mol^{-1}),[123] even though the average charge density on an aluminum in the **GaAl$_{12}$** is lower than that in the $Al(H_2O)_6^{3+}$. This deviation is striking.

Table 1. Rates of Exchange of Oxygens between Bulk Solution and μ_2-OH Bridges in the ϵ-Al_{13}, $GaAl_{12}$, and $GeAl_{12}$ Molecules[117−120,122] [a]

molecule	k_{ex}^{298} (s^{-1})	$\Delta H^{\ddagger}$ (kJ mol^{-1})	$\Delta S^{\ddagger}$ (kJ mol^{-1} K^{-1})	$\Delta V^{\ddagger}$ (cm^3 mol^{-1})
		ϵ-Al_{13}		
μ_2-OH^{fast}	$(1.6 \pm 0.4) \times 10^{-2}$	204 ± 12	403 ± 43	
μ_2-OH^{slow}	$(1.6 \pm 0.1) \times 10^{-5}$	104 ± 20	5 ± 4	
		$GaAl_{12}$		
μ_2-OH^{fast}	$(1.8 \pm 0.1) \times 10^{-5}$	98 ± 3	-8 ± 9	
μ_2-OH^{slow}	$(4.1 \pm 0.2) \times 10^{-7}$	125 ± 4	54 ± 12	$+7 \pm 1$
		$GeAl_{12}$		
μ_2-OH^{fast} [b]				
μ_2-OH^{slow}	$(6.6 \pm 0.2) \times 10^{-4}$	82 ± 2	-29 ± 7	
		Al_{30}		
	rates are similar to **$GaAl_{12}$** cluster			

[a] At the pH conditions, the molecules are fully protonated and there is no strong pH dependence for exchange rates. A small pH dependence is detectable for the **$GeAl_{12}$** molecule, which is the strongest acid in the set. [b] Complete in minutes or less.

Table 2. Rate Parameters for Exchange of Water Molecules from the Inner Coordination Sphere of Al(III) Complexes to the Bulk Solution, as Determined from ^{17}O NMR[a]

species[b]	$k_{H_2O}^{298}$ (s^{-1}) ($\pm 1\sigma$)	$\Delta H^{\ddagger}$ (kJ mol^{-1})	$\Delta S^{\ddagger}$ (J K^{-1} mol^{-1})	$\Delta V^{\ddagger}$ (cm^3 mol^{-1})
		Monomeric Complexes		
$Al(H_2O)_6^{+3}$	1.29 ± 0.03	85 ± 3	42 ± 9	$+5.7$
$Al(H_2O)_5OH^{2+}$	31000 ± 7750	36 ± 5	-36 ± 15	
$AlF(H_2O)_5^{2+}$	240 ± 34	79 ± 3	17 ± 10	
$AlF_2(H_2O)_4^{+}$	16500 ± 980	65 ± 2	53 ± 6	
$Al(ssal)^{+}$	3000 ± 240	37 ± 3	-54 ± 9	
$Al(sal)^{+}$	4900 ± 340	35 ± 3	-57 ± 11	
$Al(mMal)^{+}$	660 ± 120	66 ± 1	31 ± 2	
$Al(mMal)_2^{-}$	6900 ± 140	55 ± 3	13 ± 11	
$Al(ox)^{+}$	109 ± 14	69 ± 2	25 ± 7	
		Multimeric Complexes		
ϵ-Al_{13}	1100 ± 100	53 ± 12	-7 ± 25	
$GaAl_{12}$	227 ± 43	63 ± 7	29 ± 21	$+3 \pm 1$
$GeAl_{12}$	190 ± 43	56 ± 7	20 ± 21	

[a] The original sources can be found in refs 118−120 and 122. The $\Delta V^{\ddagger}$ value for $Al(H_2O)_5OH^{2+}$ is not reported but is consistent with a change in coordination.[136] [b] abbreviations: ox = oxalate; ssal = sulfosalicylate; sal = salicylate; mMal = methylmalonate.

Usually, reduced charge density on a trivalent metal results in a more dissociative character for solvent exchange, such as is observed when a fully protonated metal ion (e.g., $Fe(H_2O)_6^{3+}$, $\Delta V^{\ddagger} = -5.4 \pm 0.4$ cm^3 mol^{-1}, or $Ga(H_2O)_6^{3+}$, $\Delta V^{\ddagger} = +5.0 \pm 0.5$ cm^3 mol^{-1}) is compared to its first conjugate base ($Fe(H_2O)_5OH^{2+}$, $\Delta V^{\ddagger} = +7.0 \pm 0.5$ cm^3 mol^{-1}, or $Ga(H_2O)_5OH^{2+}$, $\Delta V^{\ddagger} = +6.2$ cm^3 mol^{-1}).[123−128] The difference suggests that water exchange on the larger **$GaAl_{12}$** complex has less dissociative character than the fully hydrated ion, although the average charge density is lower.

The paradox of reactivity for these ϵ-Keggin aluminum molecules is that a single atom substitution in the central $M(O)_4$ site has profound effect on the rates of exchange of μ_2-OH but not bound waters. For isotopic exchange into the bridges, the reactivity trend is **$GeAl_{12}$** > **ϵ-Al_{13}** > **$GaAl_{12}$**, and the rates differ by at least a factor of $\sim 10^5$. For the **ϵ-Al_{13}** and **$GaAl_{12}$** molecules, the data indicate that oxygen-isotope exchange from the bulk solution to the μ_2-OH sites is independent of pH, albeit over a narrow range ($4.5 < pH < 5.5$). Yet, for all hydroxyl bridges and bound waters, the exchanging oxygens are three bonds removed from the central metal.

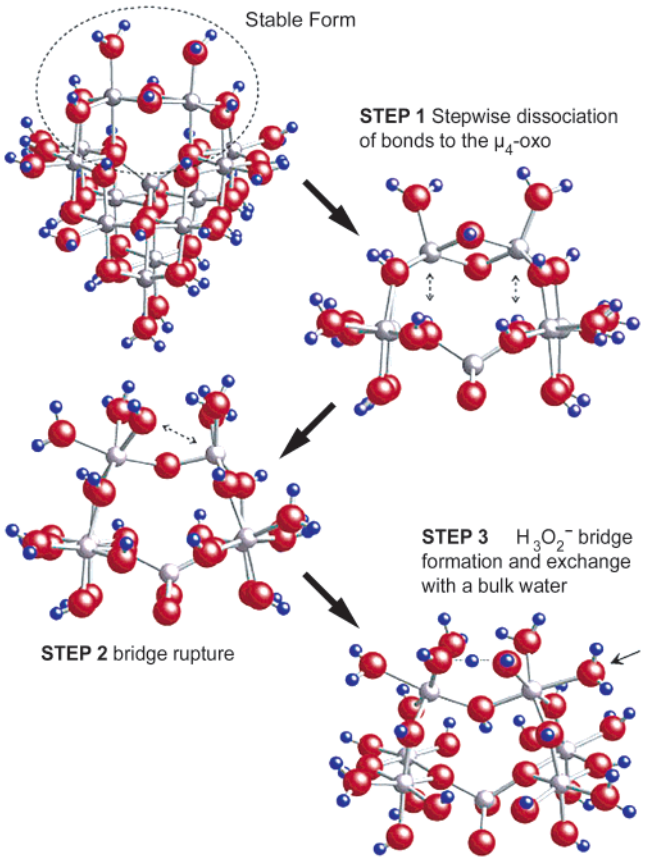

Figure 11. The rates of oxygen-isotope exchange into μ_2-OH^a and μ_2-OH^b in the **ϵ-Al_{13}**, **$GaAl_{12}$**, and **$GeAl_{12}$** vary by a factor of at least 10^5 (**$GeAl_{12}$** > **ϵ-Al_{13}** > **$GaAl_{12}$**), yet the μ_4-O sites are inert, rates are largely independent of pH, and the bound waters exchange at virtually identical rates. This paradox was explained by Rustad et al.,[129] who hypothesized from computer simulations that a metastable intermediate forms that involves partial detachment of two $Al(O)_6$ from the μ_4-O to release part of the linked structures. The resulting partly detached moiety undergoes isotopic exchange via pathways that are similar to those affecting an inert-metal dimer, which parts of it resemble. Dissociation of one μ_2-OH and hydration by a bulk water molecule forms an $H_3O_2^-$ bridge where oxygens can exchange rapidly. After the oxygens exchange positions in the $H_3O_2^-$ bridge, the reaction reverses and the partly detached structures collapses back into the stable **MAl_{12}** structure. In the Rustad et al. model,[129] this partly detached structure forms constantly at a low concentration. The steady concentration depends critically on the strength of the bond from the central metal to the μ_4-O, which explains the enormous range in reactivities. The μ_4-O, of course, remains unexchanged.

A reasonable explanation of the paradox was provided by Rustad et al.,[129] who employed molecular-dynamics simulations and ab initio calculations to come up with a pathway for oxygen-isotopic exchange that involved a partly dissociated form of each molecule. They hypothesized that two $Al(O)_6$ in the outer part of the structure detach from the μ_4-O [Figure 11], creating an $Al(\mu_2\text{-}OH)_2Al$ dimer-like structure on the molecule that interacts strongly with bulk waters and partly dissociates. As the μ_2-OH in this dimer dissociates, a $H_3O_2^-$ bridge forms [Figure 11] that can easily exchange for a bulk water, much like the transient $H_3O_2^-$ bridge that forms in dimers of trivalent metals [e.g., ref 123]. The extent to which this metastable moiety forms from the stable structure depends on the central metal and varies inversely with the strength of the M−(μ_4-O) bond. Hence the intermediate forms in the order **$GeAl_{12}$** > **ϵ-Al_{13}** > **$GaAl_{12}$**. The reaction is not proton catalyzed, and the rates are thus

independent of pH. The exchange of bound waters takes place at the stable structures so the atom in the central $M(O)_4$ site has little effect on the Al−(η-OH_2) bond strength. Thus, the rates of exchange of bound waters are largely independent of the central metal, whereas the rates of exchange of hydroxyl bridges are enormously sensitive.

The Rustad et al.[129] hypothesis, although unproven, is consistent with measurements of the $\Delta V^{\ddagger}$ value for oxygen-isotope exchange into the μ_2-OH^{slow} site in the **$GaAl_{12}$** molecule,[122] which is the only μ_2-OH for which $\Delta V^{\ddagger}$ values exist. If an expanded structure forms from the stable ϵ-Keggin structure at steady state, then one expects a large positive contribution of reaction volume to the experimental activation volume. Correspondingly, near 322 K the rates of exchange for the less labile set of bridging hydroxyls in the **$GaAl_{12}$** decrease by a factor of about two with increasing pressure from 0.1 to 350 MPa, consistent with $\Delta V^{\ddagger} = +7 \pm 1$ cm^3 mol^{-1}. This $\Delta V^{\ddagger}$ parameter would include any expansion of the molecule to form a metastable intermediate and does suggest significant bond lengthening in the reaction.

A similar set of ^{17}O NMR studies were conducted on the **Al_{30}** molecule at conditions limited to pH ≈ 4.7 and 32−40 °C.[80] Although it was impossible to determine rates for individual oxygen sites in the **Al_{30}**, the ^{17}O NMR peak positions fall into the same range as those for the **MAl_{12}** molecules. With the growth in intensities of these peaks used as a guide, rates of isotopic equilibration of the μ_2-OH, μ_3-OH, and bound water molecules fall broadly within the same range as the ϵ-**Al_{13}** and **$GaAl_{12}$** molecules. The μ_2-OH and μ_3-OH equilibrate within a couple of weeks in this temperature range, and the peak in the ^{17}O NMR spectra that is assigned to bound water molecules varies in width with temperature in a similar fashion as that for other aluminum solutes ($\tau_{ex}^{298} \approx 0.01-0.0001$ s). Thus, most of the bound waters on the **Al_{30}** probably exchange with bulk solution at rates that fall within the range observed for other aluminum complexes. However, signal from one anomalous group of four η-OH_2 sites is not observed, indicating that these sites exchange at least a factor of 10 more rapidly than the other bound waters on the **Al_{30}**.[80] Phillips et al.[80] speculated that these four waters were those cis to the μ_3-OH formed by capping the δ-**Al_{13}** units [Figure 5]. Subsequent work has shown that these caps are particularly reactive (see below).

3.3. Kinetic Data for Other Ligand Exchanges on the MAl_{12}

3.3.1. Reactions at Bound Water Molecules

The most extensive data on ligand exchanges involving the **MAl_{12}** molecules are from Forde and Hynes,[130] who employed stop-flow methods to determine the rate coefficients for reaction of a series of phenolic compounds [Scheme 1] with the ϵ-**Al_{13}**. (In Scheme 1, the set of phenols are shown above a typical reaction written with catechol.) This study is particularly important because, along with Yu et al.,[131] it establishes that the reaction rates at the large **MAl_{12}** ions proceed via familiar I_d pathways and that one can estimate rate coefficients. Some of the phenolic compounds studied by Forde and Hynes[130] are common in natural waters as breakdown products of lignin, and they bind strongly to aluminum hydroxide colloids. The authors presented a pathway that involves rapid formation of an electrostatic ion pair, followed by slow loss of a bound water and formation of a strong inner-sphere bond. The closure of the chelate

Scheme 1

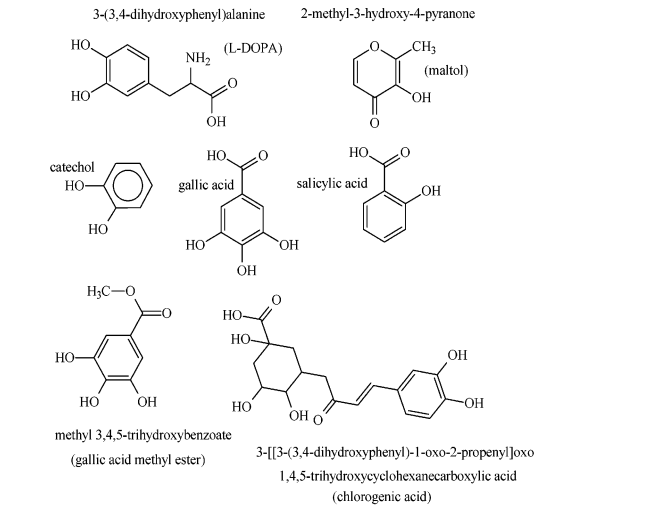

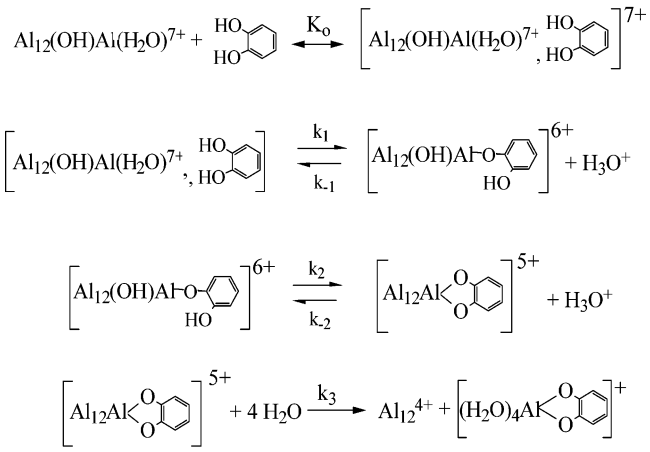

ring [Scheme 1] is relatively rapid, and the final step is rapid decomposition of the modified molecule to form aluminum−phenolate monomer complexes. This rapid decomposition is consistent with the documented instability of ϵ-**Al_{13}** in phenol-rich soil solutions (see below).

Yu et al.[131] examined pathways whereby fluoride ion replaces bound waters and hydroxyl bridges in the **$GaAl_{12}$** molecule. The first and most conspicuous reaction was replacement of a bound water molecule on the **$GaAl_{12}$** molecule:

$$GaAl_{12}^{7+} + F^- \xrightarrow{k_{F^-}^{278}} GaAlF^{6+} + H_2O \qquad (2)$$

The experimental conditions (4.0 < pH < 5.5) were chosen so that virtually all of the dissolved fluoride was present as the F^- ion, the **$GaAl_{12}$** molecule was fully protonated, and the replaceable functional groups were usually in excess of the fluoride concentration. The potentiometry indicated a first-order reaction in both fluoride and **$GaAl_{12}$**, as expected, and no pH dependence. The reaction at low temperatures (278 K) was sufficiently slow to follow using a fluoride-specific electrode [Figure 12].

Enough data exist to establish the reasonableness of the Eigen−Wilkins−Tamm mechanism for ligand exchange by comparing the measured rate coefficients with one estimated from the product of an equilibrium constant (K_{os}) for

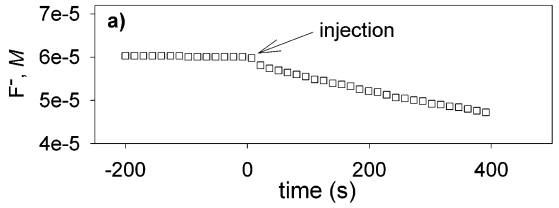

Figure 12. Changes in the concentration of dissolved fluoride in a 5 mL solution of $\sum[F] = 6 \times 10^{-5}$ M before and after injection of 0.100 mL of 1.7×10^{-3} M **GaAl$_{12}$** at pH = 4.5 and 278 K.[131] Bound waters on the **GaAl$_{12}$** molecule are replaced by fluoride ions with nearly the same rate law as that on the $Al(H_2O)_6^{3+}$(aq) ion; that is, the rates are first order in [F$^-$] and **GaAl$_{12}$** concentrations and largely controlled by the rates of solvolysis. Thus, rates of ligand substitution at the bound waters on the **MAl$_{12}$** molecules are similar to monomeric aqueous complexes [Table 3]. A slower subsequent reaction is fluoride replacement of μ_2-OH, which can be followed by ^{19}F NMR.[131,137]

formation of the outer-sphere precursor and the rate of water exchange reported for the **MAl$_{12}$**: $k^{calcd} = K_{os}k^{T}_{H_2O}$. The constant K_{os} is calculated from a version of the Fuoss equation:[128,133]

$$K_{os} = \frac{4000N\pi a^3}{3}\exp\left[\frac{-z_+z_-e^2}{4\pi\epsilon_0\epsilon kTa}\right]\exp\left[\frac{-z_+z_-e^2\kappa}{4\pi\epsilon_0\epsilon kT(1+\kappa a)}\right] \quad (3)$$

where $\kappa = \sqrt{2000\epsilon^2 NI/(\epsilon\epsilon_0 kT)}$, e is the elementary charge in coulombs, k is Boltzmann's constant in J K^{-1}, N is Avogadro's number (mol^{-1}), ϵ_0 is the vacuum permittivity (8.854×10^{-12} J^{-1} C^2 m^{-1}), ϵ is the dielectric constant of water at temperature, the parameter a is the distance of closest approach of the ions (5×10^{-10} m), T is temperature in kelvin, I is ionic strength (mol L^{-1}), and z_+ and z_- are the charges of the ions. The value of $k^{T}_{H_2O}$ is given or can be estimated from the data in Table 2.

All of the phenolic ligands used by Forde and Hynes[130] are uncharged at the experimental pH and have $K_{os} = 0.32$ M^{-1}. With use of $k^{298}_{H_2O} = 1100$ s^{-1}, the second-order rate coefficient for ligand exchange is estimated to be $k \approx 350$ M^{-1} s^{-1}. The ratios of k^{expt}/k^{calcd} vary around unity [Table 3], as expected. The experiments of Yu et al.[131] were carried

Table 3. A Summary of Kinetic Data for Reaction of Phenol Ligands with ϵ-Al$_{13}$ in Aqueous Solution at 25 °C and I = 1.0 M from ref 130 and for Reaction of Fluoride Ion with the GaAl$_{12}$ Molecule at 278 K and I = 0.6 M from ref 131

ligand	k, M^{-1} s^{-1}	k^{expt}/k^{calcd}
	ϵ-Al$_{13}$, $k^{298}_{H_2O} = 1100$ s^{-1}	
catechol	23.0 ± 0.08	0.07
L-dopa	33.3 ± 0.7	0.10
salicylic acid	119 ± 3.4	0.34
maltol	96.6 ± 3.4	0.28
gallic-acid ester	192 ± 6.8	0.55
chlorogenic acid	489 ± 16.2	1.40
	GaAl$_{12}$, $k^{278}_{H_2O} = 36$ s^{-1}	
F$^-$	7.05 ± 1.2	0.5
	Al^{3+}, $k^{298}_{H_2O} = 1.29$ s^{-1}; $K_{os} = 0.15$ M^{-1}	
F$^-$	1.55 ± 0.35	8.0

out at lower temperature (278 K) and ionic strength (I = 0.6). At these conditions, $k^{278}_{H_2O} \approx 36$ s^{-1} is estimated from the data in Table 2, and the average rate coefficient for eq 2 can be calculated from Table 2 in Yu et al.,[131] yielding $k^{278}_{F^-} = 7.05 \pm 1.2$ M^{-1} s^{-1}. To calculate the ion-pairing constant, we use the average charge on an Al(III) metal in the **GaAl$_{12}$** molecule (+0.54), rather than the +7 total ion charge, to get $K_{os} \approx 0.5$ M^{-1} or $k^{expt}/k^{calcd} \approx 0.4$, which is fully consistent with the data for the phenols[130] and consistent with an Eigen−Wilkins−Tamm mechanism. The loss of a bound water molecule controls the rate of the overall ligand-exchange reaction, and this rate is relatively unaffected by the incoming ligand.

For comparison, also included in Table 3 is the ratio k^{expt}/k^{calcd} for the reaction

$$Al^{3+} + F^- \xrightarrow{k^{298}_{F^-}} AlF^{+2} \quad (4)$$

using data from refs 133 and 134 (see also ref 216) but recalculated to be consistent with the **Al$_{13}$** and **GaAl$_{12}$** results reported here. This recalculation follows the lead of Forde and Hynes[130] and ignores the $^3/_4$ statistical factor that is typically employed and sets $a = 5 \times 10^{-10}$ m for all molecules and ligands. Given these approximations, we calculate $K_{os} = 0.15$ M^{-1} at I = 0.1 and 298 K, and $k^{expt}/k^{calcd} \approx 8.0$. This fluoridation reaction is well accepted as proceeding via an Eigen−Wilkins−Tamm mechanism and indicates that the reactions for the **MAl$_{12}$** molecules are probably also I$_d$.

By extrapolation, ligand-exchange reactions on larger molecules (see below), and perhaps even aluminum colloids, will be controlled by rates of water dissociation, which fall into the familiar millisecond range for aluminum monomers. Oxygen exchange will involve concerted motions of the entering and leaving groups, and it is unsurprising that ligand exchanges on Al(III) in these large molecules have a considerable dissociative character. As pointed out by Swaddle,[135] the ionic radius [53.5 pm] of Al(III) is smaller than the hexagonal interstices [57 pm] in an array of cubic-close-packed spheres with radii of 138 pm, that of water in ice, so aluminum is much more likely to decrease coordination to oxygens than to tolerate an increase in coordination number [e.g., ref 136]. In summary, the data for exchange of a ligand for a bound water molecule on the **MAl$_{12}$** series of molecules appear to be consistent with the results for monomers and I$_d$ mechanisms, although high-pressure data only exist for a single molecule.

3.3.2. Reactions at Bridging Hydroxyls

A striking result is the extraordinary difference in reactivity of the μ_2-OH^{fast} and μ_2-OH^{slow} sites within the **ϵ-Al$_{13}$**, **GaAl$_{12}$**, and **GeAl$_{12}$** molecules [Table 1]. Clear evidence for the different reaction rates is particularly evident in the fluoride-uptake experiments of Yu et al.[131] who followed the reaction using ^{19}F NMR and potentiometry and saw peaks in the ^{19}F NMR spectra that were assigned to both bridging (−131 to −138 ppm) and nonbridging fluorides (−148 ppm) on the **GaAl$_{12}$** molecule. The results were interpreted to indicate parallel and possibly even reversible transfer of fluoride from nonbridging sites to the two bridging sites.

The essential feature of the rate law was that fluoride replaces bound water molecules within seconds at 278 K and that the two μ_2-OH sites form more slowly and at different rates. The nonbridging fluoride peaks decrease in intensity with time as peaks assigned to the bridging fluorides increase. Notably, rates of fluoride replacement of μ_2-OH sites are 10^1-10^3 times more rapid than the rates of oxygen

exchange with bulk waters into the bridging hydroxyls. Allouche and Taulelle[137] found that fluoridation of the **Al$_{13}$** molecule accelerated conversion to other isomers (see below). Most importantly, they found that the rate of fluoridation of the **Al$_{13}$** is greater than that of the **GaAl$_{12}$**, as one expects from the rates of oxygen-exchange into the respective μ_2-OH bridges [Table 1].

Allouche and Taulelle[137] also studied fluoridated **Al$_{13}$** crystals and found peaks assignable to bridging fluorides at −132 and −134 ppm, consistent with the earlier results. Phillips et al.[138] conducted ^{19}F{^{27}Al}-transfer of populations in double resonance (TRAPDOR) experiments in fluoride-substituted **GaAl$_{12}$**−selenate crystals and found an additional peak near −124 ppm, as well as three peaks in the range −130 to −139 ppm that are assignable to the fluoridated bridges, suggesting that a richer array of ^{19}F environments can be detected with advanced spectroscopy. There is thus broad agreement between the results of fluoridation with these aluminum polyoxocations and aluminum hydroxide minerals. Site-specific reaction rates can be established that are probably relevant to environmental materials such as aluminous clays.[139]

3.3.3. Dissociation Rates and Pathways

The fact that four central μ_4-oxo sites remain isotopically normal during ^{17}O injection experiments indicates that exchange rate laws for all other atom positions in the ϵ-**Al$_{13}$**, **GaAl$_{12}$**, and **GeAl$_{12}$** molecules are measured without complete dissociation. The rates of complete dissociation of the ϵ-**Al$_{13}$** alone have been measured[140−142] and indicate that the molecule experiences many tens to hundreds of isotopic exchanges in the μ_2-OH sites before it dissociates completely. Complete dissociation of the ϵ-**Al$_{13}$** molecule is first-order in proton concentration in acidic solutions and second-order in proton concentration at pH < 2.5. The activation energies for dissolution are also relatively small (13.3 ± 1.9 and 44.9 ± 4.9 kJ mol^{-1} [140]) and vary with solution pH, indicating that there are contributions of protonation enthalpy to the temperature dependence of the reaction rate even in pH condtions (2 < pH < 3.5) that are well away from the pK_a of the bound waters (pH ≈ 6.5). Furrer et al.[140] interpreted the dominant mechanism at pH > 2.5 to involve a protonated μ_2-OH site and the mechanism at pH < 2.5, which is second-order in protons, to involve two adjacent protonated bridges.

The newer ^{17}O NMR data indicate that both the μ_2-OH^{slow} and μ_2-OH^{fast} sites exchange many times before the ϵ-**Al$_{13}$** molecule dissociates and that these exchanges are independent of pH (however at slightly higher pH conditions than the Furrer et al.[140] study). Besides the mismatch between the pH dependence of the dissolution and the pH independence of the isotope-exchange reactions, the activation energies for dissolution are much smaller than those for oxygen-isotope exchange at the hydroxyl bridges ($\Delta H^{\ddagger}$ = 104 and 204 kJ mol^{-1}, Table 1). Furthermore, because the μ_4-O remains inert even as all other oxygen sites exchange isotopes with the aqueous solution, dissociation of μ_2-OH sites cannot be key to the dissolution mechanism. One model to account for the data is that protonation of the inert μ_4-O sites, followed by hydration, causes the molecule to dissociate. Casey et al.[118] reached this conclusion largely by elimination, since the time scales for dissociating all other oxygens are too small relative to dissolution and the rate parameters (activation energies and rate orders) are too different to account for the dissolution experiments.

The pH dependencies for dissociation and μ_2-OH bridge cleavage are also wrong for these ruptures to control dissociation of the molecule. Experiments in the acid-pH direction are limited by dissolution of the molecule in lengthy experiments, and experiments in more basic solutions are difficult because the molecules irreversibly link as the pH exceeds the dissociation pH. Nevertheless, the rates of oxygen-isotope exchange between bulk solution and the **Al$_{13}$** and **GaAl$_{12}$** are independent of pH (over about 0.5 pH units) as long as pH < 6.5.[117−119] The **GeAl$_{12}$** has a clear pH dependence to the exchange rates of both the bound waters and the one set of μ_2-OH sites (μ_2-OH^{slow}) that can be studied. The pH dependence measured for oxygen-isotope exchange rates in the **GeAl$_{12}$** is because the experimentally accessible pH range is near to the pK_a value for deprotonation of the bound water molecules.[143,144] Thus, a bound hydroxyl labilizes both the bound waters and the μ_2-OH, as is observed for the fluoride-substituted **GaAl$_{12}$**, which is isoelectronic.[131]

3.3.4. Formation Pathways

The conventional model for forming the ϵ-**Al$_{13}$**, **GaAl$_{12}$**, and **GeAl$_{12}$** molecules involves the initial formation of a set of $Al_3(\mu_3\text{-}OH)(\mu_2\text{-}OH)_3(H_2O)_9^{5+}$ trimers that then link together with a tetrahedral $M(OH)_4$ ion and assemble into the ϵ-**Al$_{13}$** and **MAl$_{12}$** structures [see refs 29, 52, 61, 89, 145, and 146]. Direct data are few, but Akitt and Farthing[147] concluded that the assembling molecules were $(H_2O)_4Al(\mu_2\text{-}OH)_2(H_2O)_4^{4+}$ dimers, based largely on their existence in solution with the ϵ-**Al$_{13}$**. A stable tetramer was postulated from X-ray scattering studies by Michot et al.[62] for the ϵ-**Ga$_{13}$**. Such a tetramer must certainly form in some stage of the assembly, but neither the planar $Al(O)_6$ trimers nor the tetramer has been crystallized, and these molecules probably comprise some of the missing ^{27}Al NMR intensity in a concentrated solution [e.g., refs 67 and 147]. The trimer, in contrast, is inferred from potentiometric studies[148,149] and is assigned an appropriate stoichiometry, $Al_3(\mu_3\text{-}OH)(\mu_2\text{-}OH)_3^{5+}$.

Evidence from these potentiometric titrations indicate that the $Al_3(\mu_3\text{-}OH)(\mu_2\text{-}OH)_3^{5+}$ trimer exists in solutions at 4 < pH < 5 but never reaches a large concentration, even in concentrated aluminum solutions, probably because the trimers condense to form larger clusters. There is some spectroscopic hint of the trimers because there is sometimes a relatively narrow peak in concentrated solutions at +11 ppm in the ^{27}Al NMR spectra, particularly for solutions in which ϵ-**Al$_{13}$** is being formed or decomposed [ref 81 and unpublished data]. Assignment of this peak to the planar trimer is suggested by the similarity of the chemical shift to that of the $Al(O)_6$ of the ϵ-**Al$_{13}$** complex, which is composed of four of these trimers linked together, and the small peak width, consistent with a relatively small complex. In any case, it is clear that the ϵ-**Al$_{13}$** forms via a rapid pathway during a titration, as the yield depends on the rate of base addition[30,146] and does not reach equilibrium in a typical synthesis.

Allouche and Taullele[79] and Shafran et al.[68,69] conducted a detailed study of the ϵ-**Al$_{13}$** → **Al$_{30}$** conversion and argue that capping the ϵ-**Al$_{13}$** by an $Al(O)_6$ stabilizes the structure, which matches some new evidence for metal exchanges. The slow step involves the rotation of the cap by 60° by simultaneous rupture of the more-reactive μ_2-OH bridges, followed by monomer addition and dimerization of the δ-**Al$_{13}$**. The Allouche and Taullele[79] supposition is consistent with the Son et al.[87] observation that the $Al(O)_6$ caps on the δ-**Al$_{13}$** are particularly reactive to ligand substitution.

Remarkably, Fürrer found that a solution of ϵ-**Al$_{13}$** is metastable for at least 12 years at ambient conditions but that over this time scale, the ϵ-**Al$_{13}$** converts to the **Al$_{30}$** plus some protons [see Figure 8 in ref 81]. Clearly the elevated temperatures that are most commonly used in synthesis[64,68−70] accelerate the conversion of the ϵ-**Al$_{13}$** to the **Al$_{30}$**, but the same pathways act at ambient conditions, albeit more slowly. It would involve a substantial set of experiments, but the pH dependence of the conversion could considerably advance the field.

4. Uses and Environmental Significance of the Aqueous Aluminum Hydroxide Clusters

The ϵ-**Al$_{13}$** (and to a much lesser extent the **Al$_{30}$**) is a major constituent of the industrial chemical aluminum chlorohydrate (also referred to as polyaluminum chloride). The soluble reagent that has a ratio of OH to Al of about 2.3−2.5 has the most-common stoichiometry, $Al_2(OH)_5Cl$ [see refs 2, 150, and 151]. The ensemble of polymers in this chemical changes with aging in water [e.g., ref 152], just as in titrations [e.g., refs 68, 69, 84, and 147] and species ranging from 1000 to 10 000 Da can be inferred from size-exclusion chromatography[2,82] and reaction with size-sensitive dyes. As mentioned above, none of these larger molecules, save for the **Al$_{30}$**, can be assigned in ^{27}Al NMR. Smaller aluminum hydroxide polymers, such as trimers, are inferred experimentally [e.g., ref 147] and from calculations[153] and make up some of the broad unresolvable peak in ^{27}Al NMR spectra.

Although there are suspicions about toxicity from these products, aluminum in blood plasma is usually at a common low level even in heavy users,[154,155] although antiperspirant-induced hyperaluminemia is reported [ref 15, see also refs 156 and 157]. In no recorded case is a polymeric aluminum cluster the toxicant, although Rao and Rao[158] report ϵ-**Al$_{13}$** in excised synaptosomes from rat brains. Entry into the toxicology literature is found in the November 2001 issue of *Inorganic Biochemistry* and review articles[14,159] dealing with aluminum biochemistry and speciation in body fluids [see also ref 160].

4.1. Water Treatment

Polymeric aluminum hydroxide reagents are essential to industries, such as paper production, that release large amounts of tannins, phenols, and organic acids to wastewater [e.g., refs 13, 161, and 162]. Aluminum chlorohydrate is added to maintain large concentrations of ϵ-**Al$_{13}$** in solution, which then flocculates to form cationic sols that adsorb the organic solutes. As the flocs settle, the water is clarified, thereby improving color and taste [e.g., refs 163 and 164], and this treatment can even inactivate viruses [e.g., ref 165]. Alumino-silicate polymers are also used; although the polymer structures are unknown, they probably contain a silicate−ϵ-**Al$_{13}$** ternary complex [e.g., refs 166−168].

4.2. Pillaring Agents

The ϵ-**Al$_{13}$** molecule is among the most common pillaring agent for clays [see refs 169−173] and anionic layered solids, including titanates, manganates,[174,175] and molybdates.[176] Briefly, the ϵ-**Al$_{13}$** molecule props open the interlayer spacing of the material, which increases the microporosity [e.g., ref 177], and affects the Lewis and Brønsted acidity and proton conduction of the material [e.g., refs 178 and 179] and the ion-exchange properties [e.g., ref 179; see ref 172 for review). The pillared solid is often calcined to dehydrate the polyoxocation [e.g., ref 180], and the pillars also allow addition of interlayer dopants with particularly useful properties, such as catalytic transition-metal complexes [e.g., refs 181−184] or hydrophobic organics to pick up pollutants [e.g., ref 11]. There have been several attempts to expand the number of aluminum polyoxocations to include the **flat-Al$_{13}$**−**heidi**,[10,185] the **GaAl$_{12}$**,[6−8,186] and **Ga$_{13}$**.[6,8,187] There are literally hundreds of papers on this subject, and the interested reader is referred to refs 169−172 and 188−190 for entry into this literature.

4.3. Environmental Significance

Environmental interest in the ϵ-**Al$_{13}$** molecule stems largely from its reported phytoxicity [e.g., refs 191−194] and the potential toxicity to fish [ref 195; see also refs 196−198]. It is also considered to provide a vector for transporting pollutants[199,200] and for influencing pesticides.[201]

Natural conditions for forming the ϵ-**Al$_{13}$** molecule would be when acidic and low-organic-acid waters mix rapidly with a higher-pH solution. Such an environment could be found as dilution of acid rainfall percolating through soil into a higher-pH stream[200] or over a limestone terrain.[202] However, the critical pH window ($4.5 < pH < 6.5$) is difficult to sample during a mixing event and the ϵ-**Al$_{13}$** is suppressed by constituents common in natural waters. It dissociates rapidly by bonding to phenolic compounds[130,203−205] and metals [e.g., ref 206] and is flocculated by anions such as sulfate[166,207] or humic acids [e.g., refs 203 and 208−210]. Although there are doubts as to whether these polyoxocations exist in natural waters,[211] the ϵ-**Al$_{13}$** molecule has been detected in soil solutions,[212] and its presence is inferred from the ^{27}Al NMR spectra of pollutant floc.[200]

As mentioned earlier, the cubane-like clusters are particularly interesting because they relate closely to a hypothetical brucite packing [see ref 96]. The thermodynamically stable structure of aluminum hydroxide is gibbsite, which has six-membered rings of edge-shared $Al(O)_6$ octahedra and no μ_3-OH. This gibbsite structural arrangement is central to dioctahedral clays of trivalent metals [e.g., ref 213]. The fact that the **flat-Al$_{13}$** and **Al$_8$** molecules form quickly in concentrated aqueous solutions and that hydrotalcite phases form in dilute solutions suggests that the cubane-like structures may be stabilized in nature by substitution of divalent metals for aluminum. Synthesis of a model complex that is metastable in solution and could be used for kinetic studies would be a major advance.

5. Conclusions

In the five decades since Johansson[25−28] isolated and crystallized the ϵ-**Al$_{13}$** polyoxocation, hundreds of scientific studies have been conducted on aqueous aluminum hydroxide polyoxocations, largely because of their use as clay pillars. Interest in these aluminum clusters is resurging now because of their use as kinetic models for understanding aqueous environmental reactions. The field is reinvigorated by the persistent effort by a handful of research groups that have isolated and separated the large polymers that have long been suspected to exist in hydrolyzed aluminum solutions. The isolation and structural characterization of the δ-**Al$_{13}$**, **Al$_{30}$**, and cubane-like clusters (e.g., the **flat-Al$_{13}$**) provide new kinetic models for experiments in aqueous solutions. Furthermore, the rate at which these molecules are being found is accelerating, as the new methods of supramolecular complexation and separation help uncover clusters such as the **Ga$_{32}$**.

This work is important because these 1−2 nm aqueous clusters provide windows into the complicated processes that affect minerals and the world around us. Using the aluminum hydroxide clusters and modern spectroscopies, scientists can now follow isotope-exchange and hydrolysis reactions in ways that are impossible with aluminum hydroxide colloids, and they are uncovering surprising reactivity trends. Furthermore, the experimental results are at an appropriate scale to test algorithms of computational chemistry. Thus, experimental probing of these 1−2 nm aluminum hydroxide molecules advances our ability to predict reactive properties for many materials in water. In this sense, the aluminum polyoxocations are distinct from other polyoxometalates (e.g., tungstates) that have limited similarity to natural materials. Aluminum hydroxide substrates are everywhere in our lives, and we have little quantitative understanding as to how the form, dissolve, and react with other solutes in natural waters.

6. Acknowledgments

The author is particularly grateful to Profs. Brian Phillips and James Rustad for discussions and suggestions and to two referees who provided detailed suggestions to improve the text. Support for this research was from the Department of Energy (Grant Number DE-FG03-96ER 14629), from the American Chemical Society (PRF Grant 40412-AC2), and from the National Science Foundation (Grant EAR 0101246).

7. References

(1) Rustad, J. R. *Rev. Mineral. Geochem.* **2001**, *42*, 169.
(2) Fitzgerald, J. J.; Rosenberg, A. H. In *Antiperspirants and Deodorants*, 2nd ed.; Laden, K., Ed.; Marcel Dekker: New York, 1999; p 83.
(3) Beer, R.; Steiger, R.; Banerjee, D.; Furrer, G.; Rentsch, D.; Studer, B. Recording sheets for ink-jet printing. U.S. Patent 20050053735 to Ilford Imaging, Switzerland GmbH, 2005; 18 pp.
(4) Furrer, G.; Banerjee, D.; Rentsch, D.; Studer, B.; Beer, R. and Steiger, R. Recording sheet for ink jet printing. Eur. Pat. Appl. EP 1512544, 2005; 14 pp.
(5) van Bruggen, M. P. B.; Donker, M.; Lekkerkerker, H. N. W.; Hughes, T. L. *Colloids Surf., A* **1999**, *150*, 115.
(6) Bradley, S. M.; Kydd, R. A. *Catal. Lett.* **1991**, *8*, 185.
(7) Bradley, S. M.; Kydd, R. A. *J. Catal.* **1993**, *141*, 239.
(8) Bradley, S. M.; Kydd, R. A. *J. Catal.* **1993**, *142*, 448.
(9) Bradley, S. M., Kydd, R. A.; Brandt, K. K. *Stud. Surf. Sci. Catal.* **1992**, *73*, 287.
(10) Vicente, M. A.; Lambert, J.-F. *Clays Clay Miner.* **2003**, *51*, 168.
(11) Montargès, E.; Moreau, A.; Michot, L. J. *Appl. Clay Sci.* **1998**, *13*, 165.
(12) Bertram, R.; Gessner, W.; Müller, D.; Danner, M. *Acta Hydrochim. Hydrobiol.* **1994**, *22b*, 265.
(13) Shen, Y.-H.; Dempsey, B. A. *Environ. Int.* **1998**, *24*, 899.
(14) Gupta, R. K. *Adv. Drug Delivery Rev.* **1998**, *32*, 155.
(15) Lindblad, E. B. *Immunol. Cell Biol.* **2004**, *82*, 497.
(16) Pope, M. T. In *Comprehensive Coordination Chemistry II: From Biology to Nanotechnology*; Wedd, A. G., Ed.; Elsevier Ltd.: Oxford, U.K., 2004; Vol. 4, p 635.
(17) Hill, C. L. In *Comprehensive Coordination Chemistry-II: From Biology to Nanotechnology*; Wedd, A. G., Ed.; Elsevier: Oxford, U.K. 2004; Vol. 4, p 679.
(18) Heath, S. L.; Jordan, P. A.; Johnson, I. D.; Moore, J. R.; Powell, A. K.; Helliwell, M. *J. Inorg. Biochem.* **1995**, *59*, 785.
(19) Jordan, P. A.; Clayden, N. J.; Heath, S. L.; Moore, G. R.; Powell, A. K.; Tapparo, A. *Coord. Chem.* Rev. **1996**, *149*, 281.
(20) Seichter, W.; Mögel, H.-J.; Brand, P.; Salah, D. *Eur. J. Inorg. Chem.* **1998**, *1998*, 795.
(21) Karlsson, M. Ph.D. thesis in Chemistry, University of Umeå, Sweden, 1998.
(22) Schmitt, W.; Jordan, P. A.; Henderson, R. K.; Moore, G. R.; Anson, C. E.; Powell, A. K. *Coord. Chem. Rev.* **2002**, *228*, 115−126.
(23) Abragam, A. *The Principles of Nuclear Magnetism*; Oxford University Press: Oxford, U.K., 1961.
(24) Akitt, J. W.; Mann, B. E. *NMR and Chemistry*, 4th ed.; Stanley Thornes: New York, 2000.
(25) Johansson, G. *Acta Chem. Scand.* **1960**, *14*, 771−773.
(26) Johansson, G.; Lundgren, G.; Sillén, L. G.; Söderquist, R. *Acta Chem. Scand.* **1960**, *14*, 769.
(27) Johansson, G. *Ark. Kemi* **1963**, *20*, 305.
(28) Johansson, G. *Ark. Kemi* **1963**, *20*, 321.
(29) Akitt, J. W.; Farthing, A. *J. Chem. Soc., Dalton Trans.* **1981**, *1981*, 1624.
(30) Bottero, J. Y.; Cases, J. M.; Fiessinger, F.; Poirier, J. E. *J. Phys. Chem.* **1980**, *84*, 2933.
(31) Akitt, J. W. *Prog. NMR Spectrosc.* **1989**, *21*, 1.
(32) Bertsch, P. M.; Layton, W. J.; Barnhisel, R. I.. *Soil Sci. Soc. Am. J.* **1986**, *50*, 1449.
(33) Bertsch, P. M.; Thomas, G. W.; Barnhisel, R. I. *Soil Sci. Soc. Am. J.* **1986**, *50*, 825.
(34) Kloprogge, J. T.; Seykens, D.; Jansen, J. B. H.; Geus, J. W. *J. Non-Cryst. Solids* **1992**, *142*, 94.
(35) Kloprogge, J. T.; Seykens, D.; Geus, J. W.; Jansen, J. B. H. *J. Non-Cryst. Solids* **1992**, *142*, 87.
(36) Simpson, S. L.; Powell, K. J.; Nilsson, Nils H. S. *Anal. Chim. Acta* **1997**, *343*, 19.
(37) Bertsch, P. M.; Anderson, M. A.; Layton, W. J. *Magn. Reson. Chem.* **1989**, *27*, 283.
(38) Ferguson, J. H.; Kustin, K.; Phipps, A. *Inorg. Chim. Acta* **1980**, *43*, 49.
(39) Parker, D. R.; Bertsch, P. M. *Environ. Sci. Technol.* **1992**, *26*, 908.
(40) Parker, D. R.; Bertsch, P. M. *Environ. Sci. Technol.* **1992**, *26*, 914.
(41) Hils, A.; Grote, M.; Janssen, E.; Eichhorn, J. *Fresenius' J. Anal. Chem.* **1999**, *364*, 457.
(42) Bertsch, P. M.; Parker, D. R. In *The Environmental Chemistry of Aluminum*, 2nd ed.; Sposito, G., Ed.; CRC Press: Boca Raton, FL, 1996; p 117.
(43) Akitt, J. W.; Elders, J. M.; Letellier, P. *J. Chem. Soc., Faraday Trans.* **1987**, *83*, 1725.
(44) Baes, C. F.; Mesmer, R. E. *The Hydrolysis of Cations*; John Wiley: New York, 1976.
(45) Plyasunov, A. Y.; Grenthe, I. *Geochim. Cosmochim. Acta* **1994**, *58*, 3561.
(46) Schönherr, S.; Görz, H. *Z. Anorg. Allg. Chem.* **1983**, *503*, 37.
(47) Thomas, B.; Görz, H.; Schönherr, S. *Z. Chem.* **1987**, *27*, 183.
(48) Bradley, S. M.; Kydd, R. A.; Yamdagni, R. *J. Chem. Soc., Dalton Trans.* **1990**, *1990*, 413.
(49) Bradley, S. M.; Kydd, R. A.; Yamdagni, R. *Magn. Reson. Chem.* **1990**, *28*, 746.
(50) Bradley, S. M.; Kydd, R. A.; Yamdagni, R. *J. Chem. Soc., Dalton Trans.* **1990**, *1990*, 2653.
(51) Bradley, S. M.; Kydd, R. A.; Fyfe, C. A. *Inorg. Chem.* **1992**, *31*, 1181.
(52) Bradley, S. M.; Kydd, R. A. *J. Chem. Soc., Dalton Trans.* **1993**, *1993*, 2407.
(53) Bradley, S. M.; Lehr, C. R.; Kydd, R. A. *J. Chem. Soc., Dalton Trans.* **1993**, *1993*, 2415.
(54) Bradley, S. M.; Kydd, R. A.; Howe, R. F. *J. Colloid Interface Sci.* **1993**, *159*, 405.
(55) Bertram, R.; Schönherr, S.; Görz, H. *Z. Chem.* **1984**, *24*, 225.
(56) Görz, H.; Schönherr, S.; Pertlik, F. *Monatsh. Chem.* **1991**, *122*, 759.
(57) Lee, A. P.; Phillips, B. L.; Olmstead, M. M.; Casey, W. H. *Inorg. Chem.* **2001**, *40*, 4485.
(58) Kudynska, J.; Buckmaster, H. A.; Kawano, K.; Bradley, S. M.; Kydd, R. A. *J. Chem. Phys.* **1993**, *99*, 3329.
(59) Nagy, J. B.; Bertrand, J.-C.; Palinko, I.; Kirisci, I. *J. Chem. Soc., Chem. Commun.* **1995**, *1995*, 2269.
(60) Oszkó, A.; Kiss, J.; Kiricsi, I. *Phys. Chem. Chem. Phys.* **1999**, *1*, 2565.
(61) Parker, W. O., Jr.; Millini, R.; Kiricsi, I. *Inorg. Chem.* **1997**, *36*, 571.
(62) Michot, L. J.; Montargès-Pelletier, E.; Lartiges, B. S.; d'Espinose de la Caillerie, B.; Briois, V. *J. Am. Chem. Soc.* **2000**, *122*, 6048.
(63) Gerasko, O. A.; Mainicheva, E. A.; Naumov, D. Yu.; Kuratieva, N. V.; Sokolov, M. N.; Fedin, V. P. *Inorg. Chem.* **2005**, *44*, 4133.
(64) Fu, G.; Nazar, L. F.; Bain, A. D. *Chem. Mater.* **1991**, *3*, 602.
(65) Nazar, L. F.; Fu, G.; Bain, A. D. *J. Chem. Soc., Chem. Commun.* **1992**, *1992*, 251.
(66) Akitt, J. W.; Mann, B. E. *J. Magnet. Reson.* **1981**, *44*, 584.
(67) Akitt, J. W.; Elders, J. M.; Fontaine, X. L. R.; Kundu, A. K. *J. Chem. Soc., Dalton Trans.* **1989**, *1989*, 1889.
(68) Shafran, K. L.; Perry, C. C. *Dalton Trans.* **2005**, *2005*, 2098.
(69) Shafran, K. L.; Deschaume, O.; Perry, C. C. *Adv. Eng. Mater.* **2004**, *6*, 836.
(70) Rowsell, J.; Nazar, L. F. *J. Am. Chem. Soc.* **2000**, *122*, 3777.
(71) Allouche, L.; Gérardin, C.; Loiseau, T.; Férey, G.; Taulelle, F. *Angew. Chem., Int. Ed.* **2000**, *39*, 511.
(72) Turco, G. *Compt. Rend.* **1964**, *258*, 3331.
(73) Pauling, L. *Z. Kristallogr.* **1933**, *84*, 442.
(74) Bartl, H. *Neues Jahrb. Mineral., Monatsh.* **1970**, *12*, 552.

(75) Von Lampe, F.; Mueller, D.; Gessner, W.; Grimmer, A. R.; Scheler, G. *Z. Anorg. Allg. Chem.* **1982**, *489*, 16.
(76) Kloprogge, J. T.; Frost, R. L. *Spectrochim. Acta, Part A* **1999**, *55A*, 1505.
(77) Kunwar, A. C.; Thompson, A. R.; Gutowsky, H. S.; Oldfield, E. *J. Magn. Reson.* **1984**, *60*, 467.
(78) Zhou, B.; Sherriff, B. L.; Taulelle, F.; Wu, G. *Can. Mineral.* **2003**, *41*, 891.
(79) Allouche, L.; Taulelle, F. *Inorg. Chem. Commun*. **2003**, *6*, 1167.
(80) Phillips, B. L.; Lee, A. P.; Casey, W. H. *Geochim. Cosmochim. Acta* **2003**, *67*, 2725.
(81) Casey, W. H.; Phillips, B. L.; Furrer, G. F. *Rev. Mineral. Geochem.* **2001**, *44*, 167.
(82) Shafran, K. L.; Deschaume, O.; Perry, C. C. *J. Mater. Chem*. **2005**, *15*, 3415.
(83) Allouche, L.; Huguenard, C.; Taulelle, F. *J. Phys. Chem. Solids* **2001**, *62*, 1525.
(84) Son, J.-H.; Choi, H.; Kwon, Y.-U. *J. Am. Chem. Soc.* **2000**, *122*, 7432.
(85) Son, J.-H.; Kwon, Y.-U. *Inorg. Chem.* **2004**, *43*, 1929.
(86) Son, J.-H.; Kwon, Y.-U. *Inorg. Chim. Acta* **2005**, *358*, 310.
(87) Son, J.-H.; Kwon, Y.-U.; Han, O. H. *Inorg. Chem*. **2003**, *42*, 4153.
(88) Son, Jung-Ho; Kwon, Young-Uk. *Bull. Korean Chem. Soc.* **2001**, *22*, 1224.
(89) Jolivet, J.-P. *Metal Oxide Chemistry and Synthesis*; Wiley: New York, 2000.
(90) Cotton, F. A.; Wilkinson, G.; Murillo, C. A.; Bochmann, M. *Advanced Inorganic Chemistry*; Wiley-Interscience: New York, 1999.
(91) Akitt, J. W.; Farthing, A. *J. Chem. Soc., Dalton Trans.* **1981**, *1981*, 1624.
(92) Öhman, L.-O. *Inorg. Chem.* **1989**, *28*, 3629.
(93) Carrier, X. J.-B.; Lambert, J.-F.; Che, M. *J. Am. Chem. Soc.* **1997**, *119*, 10137.
(94) Cowan, J. J.; Bailey, A. J.; Heintz, R. A.; Do, B. T.; Hardcastle, K. I.; Hill, C. L.; Weinstock, I. A. *Inorg. Chem.* **2001**, *40*, 6666.
(95) Carrier, X.; d'Espinose de la Caillerie, J.-B.; Lambert, J.-F.; Che, M. *J. Am. Chem. Soc.* **1999**, *121*, 3377.
(96) Goodwin, J. C.; Teat, S. J.; Heath, S. C. *Angew. Chem., Int. Ed*. **2004**, *43*, 4037.
(97) Casey, W. H.; Olmstead, M. M.; Phillips, B. L. *Inorg. Chem.* **2005**, *44*, 4888.
(98) Breuil, H. *Ann. Chim. (Paris)* **1965**, *10*, 467.
(99) Powell, A. K.; Heath, S. L. *Coord. Chem. Rev.* **1996**, *149*, 59.
(100) Heath, S. L.; Jordan, P. A.; Johnson, I. D.; Moore, G. R.; Powell, A. K.; Helliwell, M. *J. Inorg. Biochem.* **1995**, *59*, 785.
(101) Schmitt, W.; Baissa, E.; Mandel, A.; Anson, C. E.; Powell, A. K. *Angew. Chem.* **2001**, *40*, 3578.
(102) Feng, T. L.; Gurian, P. L.; Healy, M. D.; Barron, A. R. *Inorg. Chem*. **1990**, *29*, 408.
(103) Pasynkiewicz, S. *Polyhedron* **1990**, *9*, 429.
(104) Roesky, H. W.; Walawalkar, M. G.; Murugavel, R. *Acc. Chem. Res.* **2001**, *34*, 201.
(105) Landry, C. C.; Pappé, N.; Mason, M. R.; Apblett, A. W.; Tyler, A. N.; MacInnes, A. N.; Barron, A. R. *Mater. Chem.* **1995**, *5*, 331.
(106) Bethley, C. E.; Aitken, C. L.; Harlan, C. J.; Koide, Y.; Bott, S. G.; Barron, A. R. *Organometallics* **1997**, *16*, 329.
(107) Koide, Y.; Barron, A. R. *Organometallics* **1995**, *14*, 4026.
(108) Callender, R. L.; Harlan, C. J.; Shapiro, N. M.; Jones, C. D.; Callahan, D. L.; Wiesner, M. R.; MacQueen, D. B.; Cook, R.; Barron, A. R. *Chem. Mater.* **1997**, *9*, 2418.
(109) Narayanan, R.; Laine, R. M. *J. Mater. Chem*. **2000**, *10*, 2097.
(110) Drljaca, A.; Hardie, M. J.; Raston, C. L. *J. Chem. Soc., Dalton Trans.* **1999**, *1999*, 3639.
(111) Hardie, M. J.; Raston, C. L. *J. Chem. Soc., Dalton. Trans.* **2000**, *2000*, 2483.
(112) Rather, E.; Gatlin, J. T.; Nixon, P. G.; Tsukamoto, T.; Kravtsov, V.; Johnson, D. W. *J. Am. Chem. Soc.* **2005**, *127*, 3242.
(113) Hiemstra, T.; Yong, H.; Van Riemsdijk, W. H. *Langmuir* **1999**, *15*, 5942.
(114) Sposito, G. *The Surface Chemistry of Natural Particles*; Oxford University: Oxford, U.K., 2004.
(115) Swift, T. J.; Connick, R. E. *J. Chem. Phys.* **1962**, *37*, 307.
(116) Thompson, A. R.; Kunwar, A. C.; Gutowsky, H. S.; Oldfield, E. *J. Chem. Soc., Dalton Trans.* **1987**, *1987*, 2317.
(117) Phillips, B. L.; Casey, W. H.; Karlsson, M. *Nature* **2000**, *404*, 379.
(118) Casey, W. H.; Phillips, B. L.; Karlsson, M.; Nordin, S.; Nordin, J. P.; Sullivan, D. J.; Neugebauer-Crawford, S. *Geochim. Cosmochim. Acta* **2000**, *64*, 2951.
(119) Casey, W. H.; Phillips, B. L. *Geochim. Cosmochim. Acta* **2001**, *65*, 705.
(120) Lee, A. P.; Phillips, B. L.; Casey, W. H. *Geochim. Cosmochim. Acta* **2002**, *66*, 577.
(121) Springborg, J. *Adv. Inorg. Chem.* **1988**, *32*, 55.
(122) Loring, J. S.; Yu, P.; Phillips, B. L.; Casey, W. H. *Geochim. Cosmochim. Acta* **2004**, *68*, 2791.
(123) Helm, L.; Merbach, A. E. *Chem. Rev.* **2005**, *105*, 1923.
(124) Hugi-Cleary, D.; Helm, L.; Merbach, A. E. *Helv. Chim. Acta* **1985**, *68*, 545.
(125) Hugi-Cleary, D.; Helm, L.; Merbach, A. E. *J. Am. Chem. Soc.* **1987**, *109*, 4444.
(126) Swaddle, T. W.; Merbach, A. E. *Inorg. Chem.* **1981**, *20*, 4212.
(127) Grant, M.; Jordan, R. B. *Inorg. Chem.* **1981**, *20*, 55.
(128) Richens, D. T. *The Chemistry of Aqua Ions*; John-Wiley: New York, 1997.
(129) Rustad, J. R.; Loring, J. S.; Casey, W. H. *Geochim. Cosmochim. Acta* **2004**, *68*, 3011.
(130) Forde, S.; Hynes, M. J. *New J. Chem.* **2002**, *26*, 1029.
(131) Yu, P.; Lee, A. P.; Phillips, B. L.; Casey, W. H. *Geochim. Cosmochim. Acta* **2003**, *67*, *1065*.
(132) Margerum, D. W.; Cayley, G. R.; Weatherburn, D. C.; Pagenkopf. G. K. In *Coordination Chemistry*; Martell, A., Ed.; ACS Monograph 174, American Chemical Society: Washington, DC, 1978; Vol. 2, p 1.
(133) Plankey, B. J.; Patterson, H. H.; Cronan, C. S. *Environ. Sci. Technol.* **1986**, *20*, 160.
(134) Plankey, B. J.; Patterson, H. H. *Inorg. Chem.* **1989**, *28*, 4331.
(135) Swaddle, T. W. *Inorg. Chem.* **1980**, *19*, 3203.
(136) Swaddle, T. S.; Rosenqvist, J. R.; Yu, P.; Bylaska, E.; Phillips, B. L.; Casey, W. H. *Science* **2005**, *308*, 1450.
(137) Allouche, L.; Taulelle, F. *Chem. Commun.* **2003**, *2003*, 2084.
(138) Phillips, B. L.; Lee, A. P.; Casey, W. H. In *Proceedings of the 11th Annual Water-Rock Interaction Conference*; Wanty, R. B., Seal, R. S., Eds.; A. A. Balkema Publishers: Leiden, The Netherlands, 2004; p 629.
(139) Nordin, J. P.; Sullivan, D. J.; Phillips, B. L.; Casey, W. H. *Geochim. Cosmochim. Acta* **1999**, *63*, 3513.
(140) Furrer, G.; Gfeller, M.; Wehrli, B. *Geochim. Cosmochim. Acta* **1999**, *63*, 3069.
(141) Amirbahman, A.; Gfeller, M.; Furrer, G. *Geochim. Cosmochim. Acta* **2000**, *64*, 911.
(142) Wehrli, B.; Wieland, E.; Furrer, G. *Aquat. Sci.* **1990**, *52*, 3.
(143) Lee, A. P.; Furrer, G.; Casey, W. H. *J. Colloid Interface Sci*. **2002**, *250*, 269.
(144) Furrer, G.; Ludwig, Chr.; Schindler, P. W. *J. Colloid Interface Sci*. **1992**, *149*, 56.
(145) Bi, S.; Wang, C.; Qing, C.; Zhang, C. *Coord. Chem. Rev.* **2004**, *248*, 441.
(146) Bertsch, P. M. *Soil Sci. Soc. Am. J.* **1987**, *51*, 825.
(147) Akitt, J. W.; Farthing, A. *J. Chem. Soc., Dalton Trans.* **1981**, *1981*, 1617.
(148) Öhman, L.-O.; Forsling, W. *Acta Chem. Scand.* **1981**, *A35*, 795.
(149) Hedlund, T.; Sjöberg, S.; Öhman, L.-O. *Acta Chem. Scand.* **1987**, *A41*, 197.
(150) Teagarden, D. L.; Kozlowski, J. F.; White, J. L.; Hem, S. L. Aluminum chlorohydrate 1: structure studies. *Pharm. Sci.* **1981**, *70*, 758−761.
(151) Teagarden, D. L.; Radavich, J. F.; White, J. L.; Hem. S. L. *Pharm. Sci.* **1981**, *70*, 762.
(152) Wang, W.-Z.; Hsu, P. H. *Clays Clay Miner.* **1994**, *42*, 356.
(153) Pophristic, V.; Klein, M. L.; Holerca, M. N. *J. Phys. Chem. A* **2004**, *108*, 113.
(154) Flarend, R. E.; Bin, T.; Elmore, D.; Hem. S. L. *Food Chem. Toxicol.* **2001**, *39*, 163.
(155) Flarend, R. E.; Hem, S. L.; White, J. L.; Elmore, D.; Suckow, M. A.; Rudy, A. C.; Dandashli, E. A. *Vaccine* **1997**, *15*, 1314.
(156) Guillard, O.; Fauconneau, B.; Olichon, D.; Dedieu, G.; Deloncle, R. *Am. J. Med.* **2004**, *117*, 956.
(157) Exley, C. *Am. J. Med.* **2004**, *117*, 969.
(158) Rao, G. V.; Rao, K. S. *FEBS* **1992**, *331*, 49.
(159) Yokel, R. A.; McNamara, P. J. *Pharmacol. Toxicol.* **2001**, *88*, 159.
(160) Harris, W. R.; Berthon, G.; Day, J. P.; Exley, C.; Flaten, T. P.; Forbes, W. F.; Kiss, T.; Orvig, C.; Zatta, P. F. *J. Toxicol. Environ. Health* **1996**, *48*, 543.
(161) Buffle, J.; Parthasarathy, N.; Haerdi, W. *Water Res.* **1985**, *19*, 7.
(162) Annadurai, G.; Sung, S. S.; Lee, D.-J. *Adv. Environ. Res.* **2004**, *8*, 713.
(163) Snodgrass, W. J.; Clark, M. M.; O'Melia, C. R. *Water Res.* **1984**, *18*, 479.
(164) O'Melia, C. R. *Water Sci. Technol.* **1998**, *37*, 129.
(165) Matsui, Y.; Matsushita T.; Sakuma S.; Gojo T.; Mamiya T.; Suzuoki H.; Inoue T. *Environ. Sci. Technol.* **2003**, *37*, 5175.
(166) Boisvert, J.-P.; Jolicoeur, C. *Colloids Surf., A* **1999**, *155*, 161.
(167) Kloprogge, J. T.; Ruan, H.; Frost, R. L. *Spectrochim. Acta* **2000**, *A56*, 2405.
(168) Gao, B. Y.; Hahn, H. H.; Hoffmann, E. *Water Res.* **2002**, *36*, 3573.

(169) Schoonheydt, R. A.; Jacobs, K. Y. In *Natural Microporous Materials in Environmental Technology*; Misaelides, P., Macá×f0ek, F., Pinnavaia, T. J., Colella, C., Eds.; NATO Science Series E, Vol. 362; Kluwer Academic Publishers: Boston, 1999; p 19.
(170) Schoonheydt, R. A.; Pinnavaia, T., Lagaly; Gangas, N. *Pure Appl. Chem.* **1999**, *71*, 2367.
(171) Schoonheydt, R. A.; Jacobs, K. Y. *Stud. Surf. Sci. Catal.* **2001**, *137*, 299.
(172) Pinnavaia, T. J. *Science* **1983**, *220*, 365.
(173) Pinnavaia, T. J.; Tzou, M.-S.; Landau, S. D.; Raythatha, R. H. *J. Mol. Catal.* **1984**, *27*, 195.
(174) Wang, L.; Ebina, Y.; Takada, K.; Kurashima, K.; Sasaki, T. *Adv. Mater.* **2004**, *16*, 1412.
(175) Wang, L.; Sakai, N.; Ebina, Y.; Takada, K.; Sasaki, T. *Chem. Mater.* **2005**, *17*, 1352.
(176) Lalik, E.; Kolodziejski, W.; Lerf, A.; Klinowski, J. *J. Phys. Chem.* **1993**, *87*, 223.
(177) Occelli, M. L.; Bertrand, J. A.; Gould, S. A. C.; Dominguez, J. M. *Microporous Mesoporous Mater.* **2000**, *34*, 195.
(178) Jones, D. J.; Leloup, J.-M.; Ding, Y.; Rozière, J. *Solid State Ionics* **1993**, *1993*, 117.
(179) Bergaoui, L.; Mrad, I.; Lambert, J.-F.; Ghorbel, A. *J. Phys. Chem. B* **1999**, *103*, 2897.
(180) Ge, Z.; Li, D.; Pinnavaia, T. J. *Microporous Mater.* **1994**, *3*, 165.
(181) Yamada, H.; Azuma, N.; Kevan, L. *J. Phys. Chem.* **1995**, *99*, 2110.
(182) Butruille, J.-R.; Michot, L. J.; Barrès, O.; Pinnavaia, T. J. *J. Catal.* **1993**, *139*, 664.
(183) Thomas, S. M.; Betrand, J. A.; Occelli, M. L.; Huggins, F.; Gould, S. A. C. *Inorg. Chem.* **1999**, *38*, 2098.
(184) Thomas, S. M.; Betrand, J. A.; Occelli, M. A. *Chem. Mater.* **1999**, *11*, 184.
(185) d'Espinose de la Caillerie, J.-B.; Man, P. P.; Vicente, M. A.; Lambert, J.-F. *J. Phys. Chem. B* **2002**, *106*, 4133.
(186) Benito, I.; del Riego, A.; Martínez, M.; Blanco, C.; Pesquera, C.; González, C. *Appl. Catal.* **1999**, *180*, 175.
(187) Montargès, E.; Michot, L. J.; Ildefonse, P. *Microporous Mesoporous Mater.* **1999**, *28*, 83.
(188) Clearfield, A. *Adv. Catal. Nanostruct. Mater.* **1996**, *1996*, 345.
(189) Cheng, S. *Catal. Today* **1999**, *49*, 303.
(190) Schoonheydt, R. A.; Leeman, H.; Scorpion, A.; Lenotte, I.; Grobet, P. *Clays Clay Miner.* **1994**, *42*, 518.
(191) Shann, J. R.; Bertsch, P. M. *Soil Sci. Soc. Am. J.* **1993**, *57*, 116.
(192) Masion, A.; Bertsch, P. M. *Plant, Cell Environ.* **2004**, *20*, 504.
(193) Parker, D. R.; Kinraide, T. B.; Zelasny, L. W. *Soil Sci. Soc. Am. J.* **1988**, *52*, 438.
(194) Parker, D. R.; Kinraide, T. B.; Zelasny, L. W. *Soil Sci. Soc. Am. J.* **1989**, *53*, 789.
(195) Flaten, T. P.; Garruto, R. M. *J. Theor. Biol.* **1992**, *156*, 417.
(196) Exley, C.; Chappel, J. S.; Birchall, J. D. *J. Theor. Biol.* **1991**, *151*, 417.
(197) Exley, C.; Wicks, A. J.; Hubert, R. B.; Birchall, D. J. *J. Theor. Biol.* **1994**, *167*, 415.
(198) Exley, C.; Wicks, A. J.; Hubert, R. B.; Birchall, D. J. *J. Theor. Biol.* **1996**, *179*, 25.
(199) Lothenbach, B.; Furrer, G.; Schulin, R. *Environ. Sci. Technol.* **1997**, *31*, 1452.
(200) Furrer, G.; Phillips, B. L.; Ulrich, K.-U.; Pöthig, R.; Casey, W. H. *Science* **2002**, *297*, 2245.
(201) Dubbin, W. E.; Sposito, G. *Environ. Sci. Technol.* **2005**, *39*, 2509.
(202) Furrer, G.; Trusch, B.; Mueller, Chr. *Geochim. Cosmochim. Acta* **1992**, *56*, 3831.
(203) Hiradate, S.; Yamaguchi, N. U. *J. Inorg. Biochem.* **2003**, *97*, 26.
(204) Masion, A.; Thomas, F.; Tchoubar, D.; Bottero, J. Y.; Tekely, P. *Langmuir* **1994**, *10*, 4353.
(205) Krishnamurti, G. S. R.; Wang, M. K.; Huang, P. M. *Clays Clay Miner.* **2004**, *52*, 734.
(206) Zhang, P.; Hahn, H. H.; Hoffmann, E.; Zeng, G. *Chemosphere* **2004**, *57*, 1489.
(207) Kerven, G. L.; Larsen, P. L.; Blamey, F. P. C. *Soil Sci. Soc. Am. J.* **1995**, *59*, 765.
(208) Masion, A.; Thomas, F.; Tchoubar, D.; Bottero, J. Y.; Tekely, P. *J. Non-Cryst. Solids* **1994**, *171*, 191.
(209) Masion, A.; Vilge-Ritter, A.; Rose, J.; Stone, W. E. E.; Teppen, B. J.; Tybacki, D.; Bottero, J.-Y. *Environ. Sci. Technol.* **2000**, *34*, 3242.
(210) Yamaguchi, N.; Hiradate, S.; Mizoguchi, M.; Miyazaki, T. *Soil Sci. Soc. Am. J.* **2004**, *68*, 1838.
(211) Gerard, F.; Boudot, J.-P.; Ranger, J. *Appl. Geochem.* **2001**, *16*, 513.
(212) Hunter, D.; Ross, D. S. *Science* **1991**, *251*, 1056.
(213) Casey, W. H.; Swaddle, T. W. *Rev. Geophys.* **2003**, *41*, 1.
(214) Baker, L. C. W.; Figgis, J. S. *J. Am. Chem. Soc.* **1970**, *92*, 3794.
(215) Chen, Y.-G.; Qu, L.-Y.; Peng, J.; Yu, M.; Lin, Y.-H.; Yu, Z.-L. *Jiegon Huaxue* **1993**, *12*, 338.
(216) Bodor, A.; Tóth, T.; Bányai, I.; Szabó, Z.; Hefter, G. T. *Inorg. Chem.* **2000**, *39*, 2530.

CR040095D